Final Report

November 2020 – June 2021

Pilot studies on GP level Crop yield estimation using Technology (Rabi 2020-21) using Sentinel 1&2 Satellite data for Rice and Wheat

Submitted to

Mahalanobis National Crop Forecast Center

ICRISAT INTERNATIONAL CROPS RESEARCH INSTITUTE FOR THE SEMI-ARID TROPICS

Pilot studies on GP level Crop yield estimation using Technology (Rabi 2020-21) using Sentinel 1&2 Satellite data for Rice and Wheat

Submitted to

Mahalanobis National Crop Forecast Center

Executing Agency	:	International Crops Research Institute for the Semi-Arid Tropics (ICRISAT) Patancheru 502 324, Telangana, India Fax : + (91) 40 30713074/30713075 Phone : + (91) 40 30713466/30713071 Email : icrisat@cgiar.org
Partner Institution	:	Mahalanobis National Crop Forecast Centre Near Krishi Vistar Sadan Pusa Campus, New Delhi-110012, India Email ncfc@gov.in
Project PI	:	Dr Murali Krishna Gumma

Project Start	:	November 2020
Project Completion	:	June 2021

Executive Summary

The Government of India plans to optimize Crop Cutting Experiments (CCEs) and Gram Panchayat crop yield estimations using different technologies including satellite derived metrics and crop modelling techniques. The present study for Rabi season (2020-21) aims to Rice and wheat crop yield estimations in 25 districts of eight states viz. Andhra Pradesh, Gujarat, Karnataka, Madhya Pradesh, Odisha, Telangana, Uttar Pradesh and Uttarakhand. The study will use comprehensive and existing environmental, weather and management data along with satellite derived crop spatial data. This information will be modelled using statistical optimization techniques and DSSAT crop modelling to assess the yield estimations.

The project will be executed by ICRISAT in partnership with Mahalanobis National Crop Forecasting Center (Ministry of Agriculture, India)

Objectives:

1. Rice and Wheat Crop extent mapping for the respective study districts
2. Conduct and assess crops cutting experiments using spatial statistical optimising technique for Rice and Wheat crop of *Rabi* season in the study districts.
3. Crop yield estimation based on DSSAT crop simulations.

Target Areas:

The pilot study allocated following twenty five districts in seven states for gram panchayat level crop yield estimation for Rice and Wheat crop (Table 1).

Table 1: Allocated districts and their respective crops for pilot study

State	District	Crop
Andhra Pradesh	Nellore	Rice
	West Godavari	Rice
Gujarat	Ahmedabad	Wheat
	Aravali	Wheat
	Sabar kantha	Wheat
Karnataka	Bellary	Rice
	Davangere	Rice
	Raichur	Rice
Madhya Pradesh	Chhatarpur	Wheat
	Raisen	Wheat
	Sagar	Wheat
	Shivpuri	Wheat
	Vidisha	Wheat
Odisha	Baleshwar	Rice
	Baragarh	Rice
	Kalahandi	Rice
Telangana	Nalgonda	Rice
	Nizamabad	Rice
	Suryapet	Rice
Uttar Pradesh	Bahraich	Wheat
	Bara banki	Wheat
	Bareilly	Wheat
	Deoria	Wheat
	Fatehpur	Wheat
Uttarakhand	Udham singh Nagar	Wheat

ICRISAT: Project implementation, monitoring, coordination and reporting

Rice and Wheat Crop mapping - Methodology

The process began with preparing NDVI maximum images for every 15 days of every month from *Rabi* season and stacked together and the crop mask was prepared using sentinel-1 VH-min by giving threshold value of greater than -25 for easy extraction of croplands as well as transplant rice fields in Google Earth Engine (GEE) Platform.

The NDVI images was prepared using normalised difference of Near Infrared (NIR) and Red (R) bands of Sentinel 2.

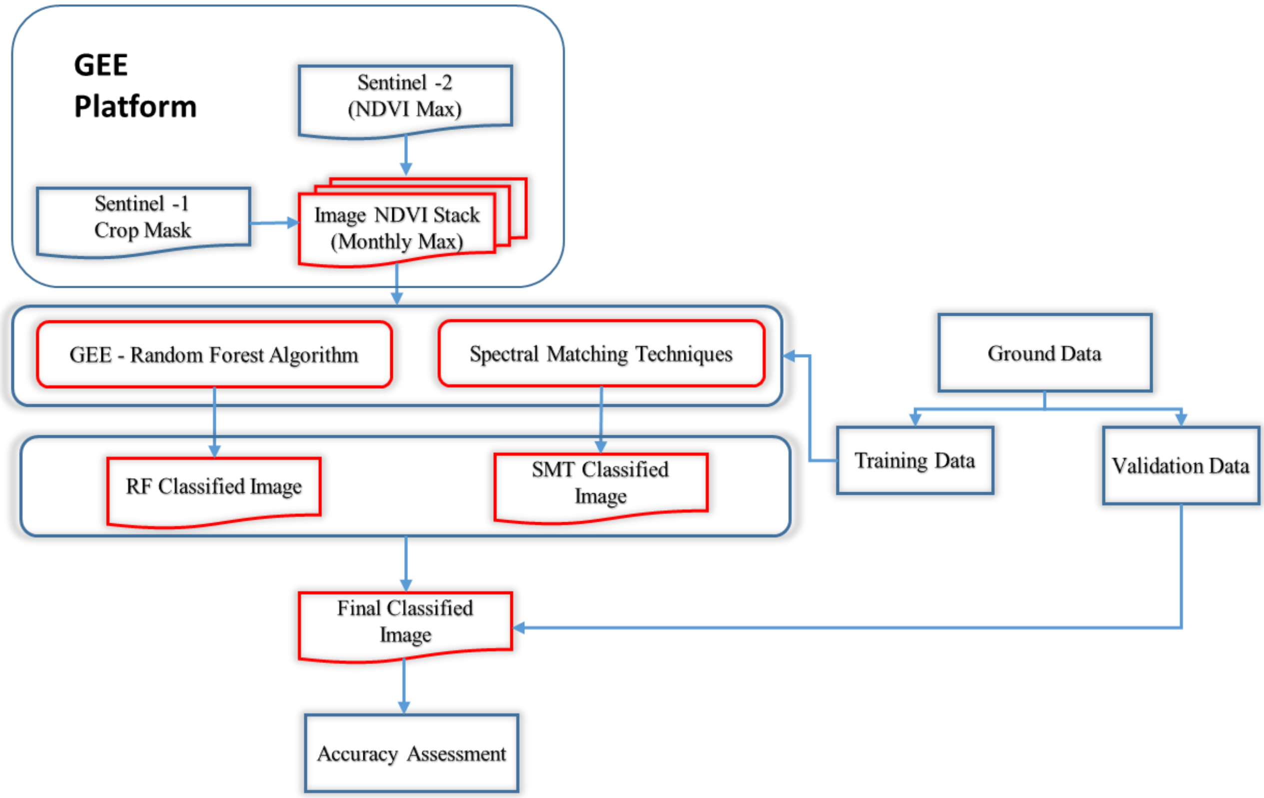

Fig 1: Flow Chart of Methodology of crop mapping

The crop mask was applied on sentinel-2 NDVI stack and classified using Random forest algorithm using training ground data.

Spectral Matching Techniques:

The stacked image downloaded from GEE consists of every 15 days for entire *Rabi* season(Murali Krishna Gumma, Thenkabail, Teluguntla, & Whitbread, 2018; Murali Krishna Gumma et al., 2019). Unsupervised classification was used to generate initial classes. The unsupervised ISOCLASS cluster algorithm (ISODATA in ERDAS Imagine 2018) run on the stack generated an initial 40 classes, with a maximum of 40 iterations and convergence threshold of 0.99. Though ground survey data was available at the time of image classification, unsupervised classification was used in order to capture the complete effect of all wavelengths over a large area. Use of unsupervised techniques is recommended for large areas that cover a wide and unknown range of vegetation types, and where landscape heterogeneity complicates identification of homogeneous training sites. Identification of training sites is particularly problematic for small, heterogeneous irrigated areas.

Land use/land cover classes were identified based on temporal signatures along with ground survey data. We observed crop growth stages including length of growing periods (LGPs) and cropping pattern from temporal signatures, such as (a) onset of cropping season (e.g., monsoon and winter); (b) duration of cropping season such as monsoon and winter; (c) magnitude of crops during different seasons and years (e.g., water stress and normal years); and (d) end of cropping season.

The process of labelling and class identification was done based on spectral matching techniques (SMTs) (Murali Krishna Gumma, Thenkabail, Deevi, et al., 2018; Murali Krishna Gumma et al., 2016; Murail Krishna Gumma, Uppala, Mohammed, Whitbread, & Mohammed, 2015). Initially, 40 classes from the unsupervised classification were grouped based on spectral similarity or closeness of class signatures. Each group of classes was matched with ideal spectral signatures and ground survey data, and assigned class names. Classes with similar time series and land cover were merged into a single class, and classes showing significant mixing, e.g., homogeneous irrigated areas and forest, were masked and reclassified using the same ISOCLASS algorithm. This resulted in following classes for each district. We employed a user-intensive method that incorporates both ground survey data and high resolution imagery in order to avoid lumping classes that might be spectrally similar but have distinct land cover(Murali Krishna Gumma et al., 2020).

Following are the crop type classification images for all study districts (Fig 2):

Andhra Pradesh

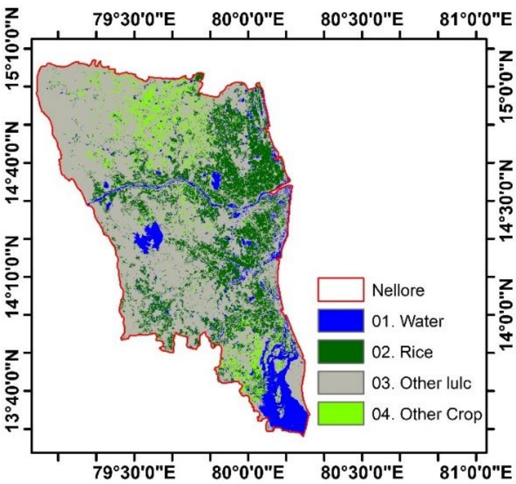

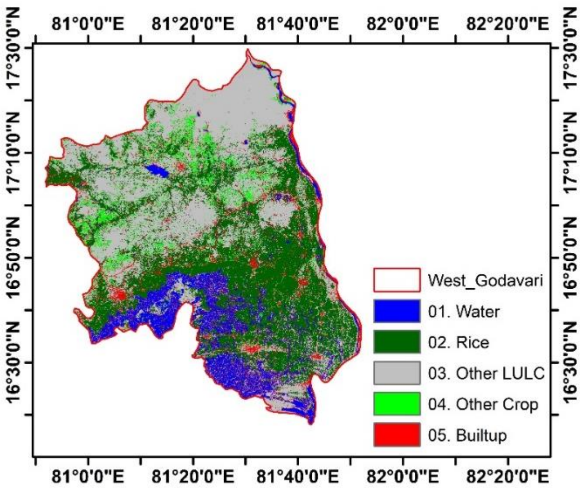

Gujarat

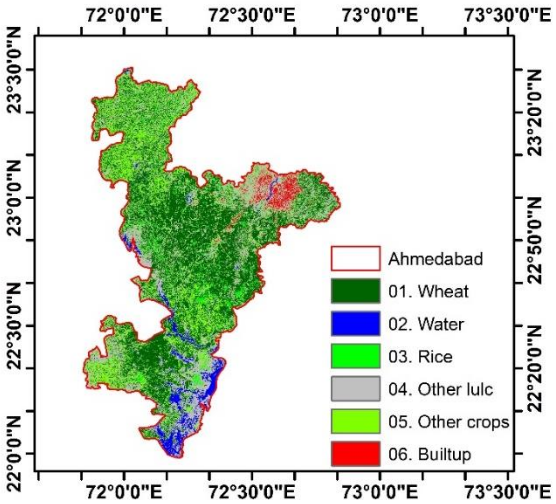

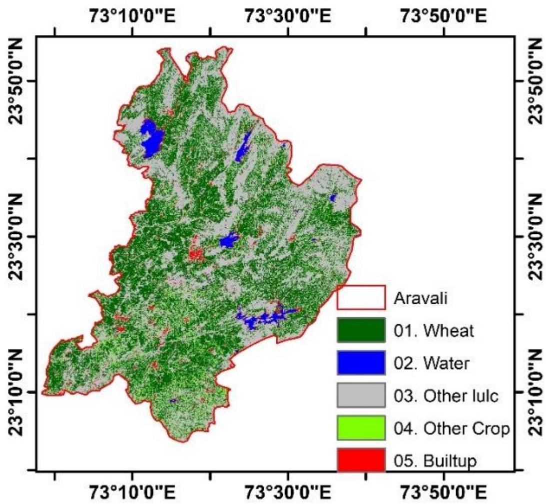

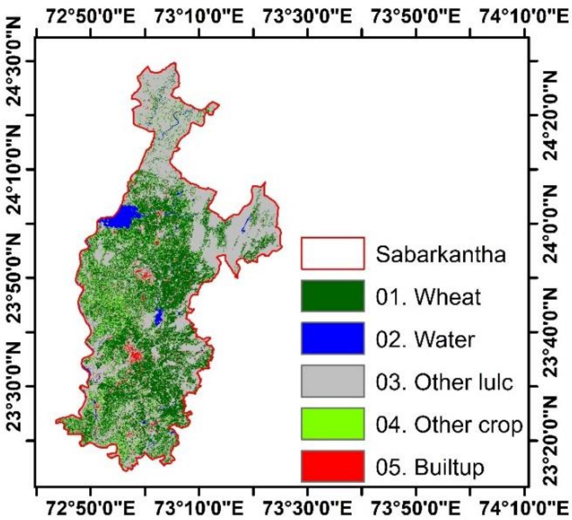

Karnataka

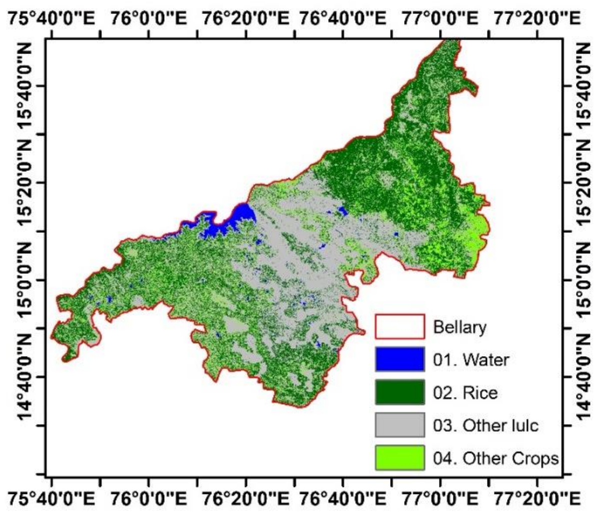

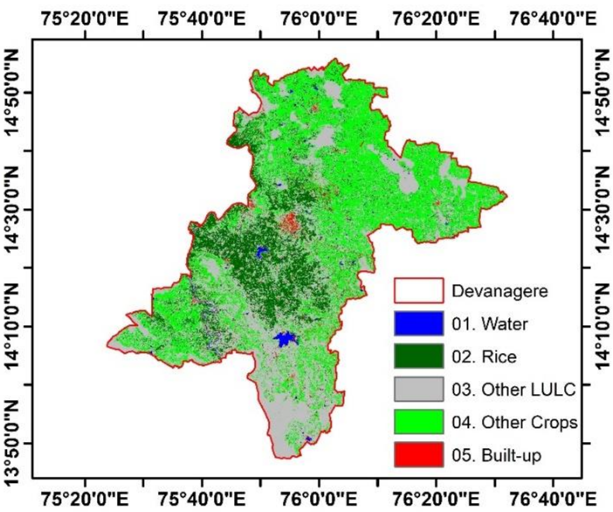

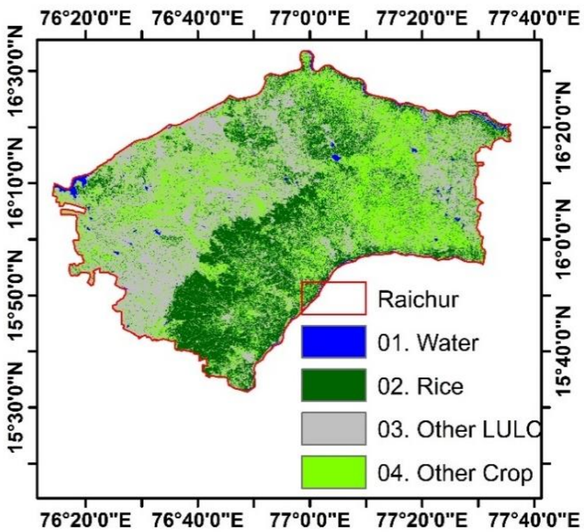

Madhya Pradesh

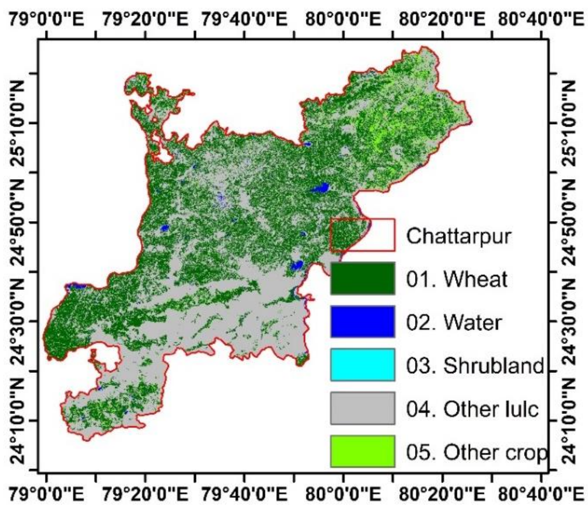

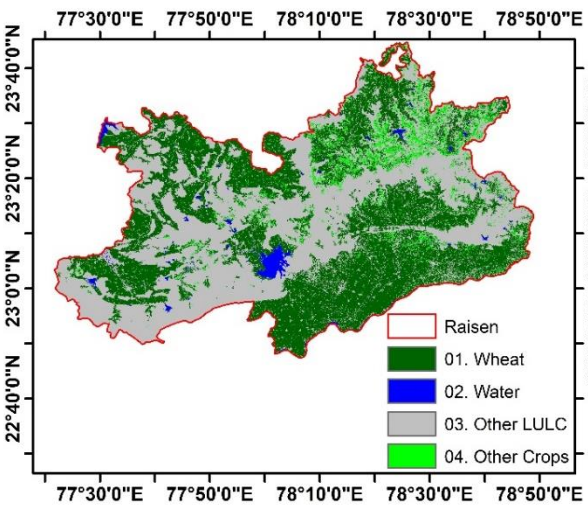

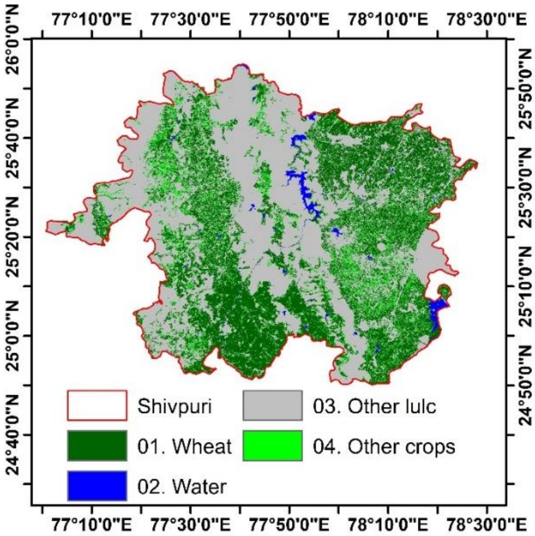
Shivpuri
01. Wheat
02. Water
03. Other lulc
04. Other crops

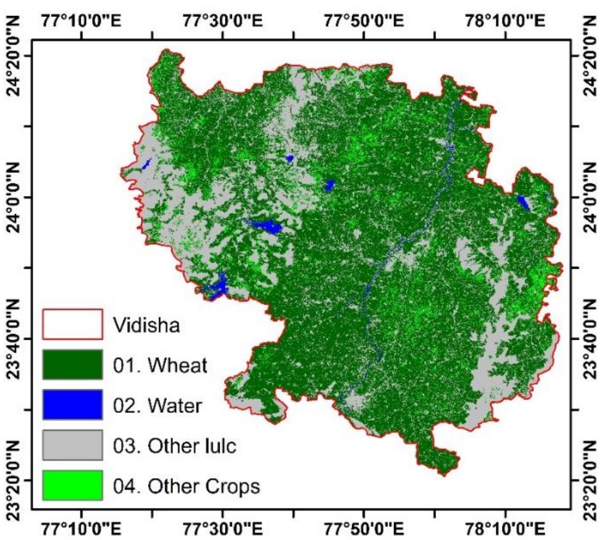
Vidisha
01. Wheat
02. Water
03. Other lulc
04. Other Crops

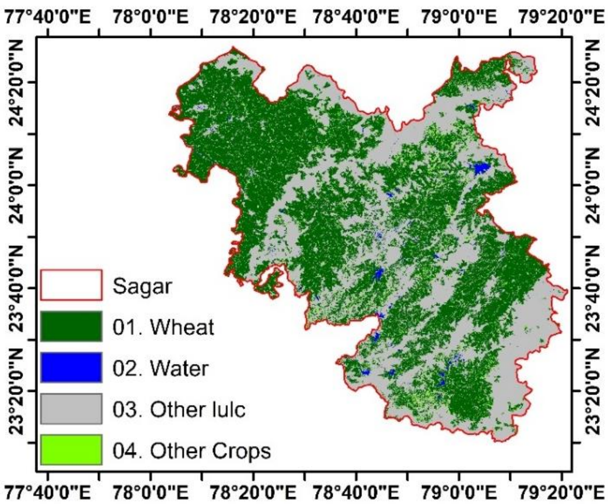
Sagar
01. Wheat
02. Water
03. Other lulc
04. Other Crops

Odisha

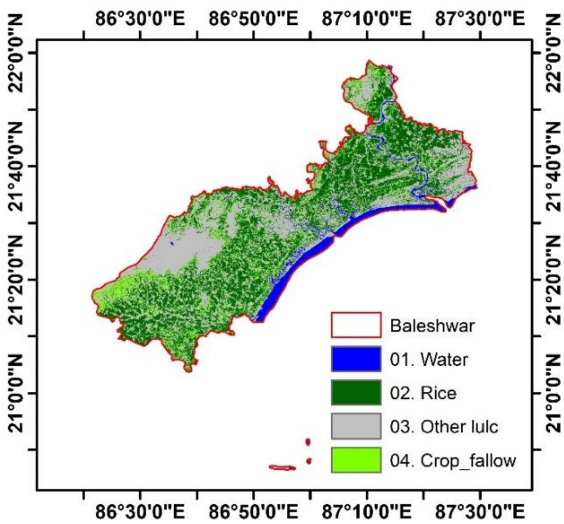
Baleshwar
01. Water
02. Rice
03. Other lulc
04. Crop_fallow

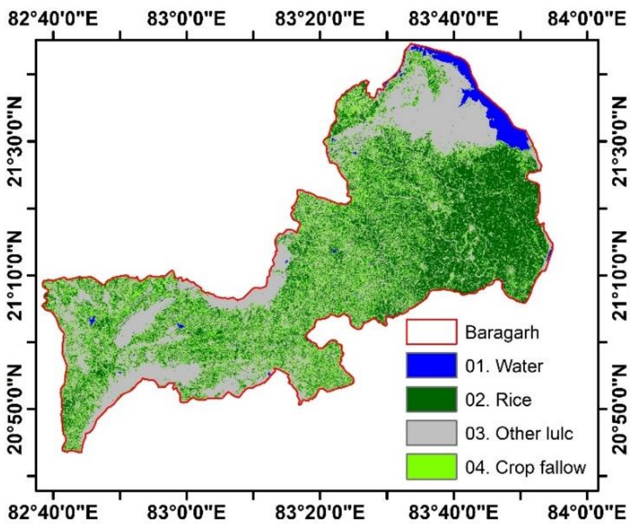
Baragarh
01. Water
02. Rice
03. Other lulc
04. Crop fallow

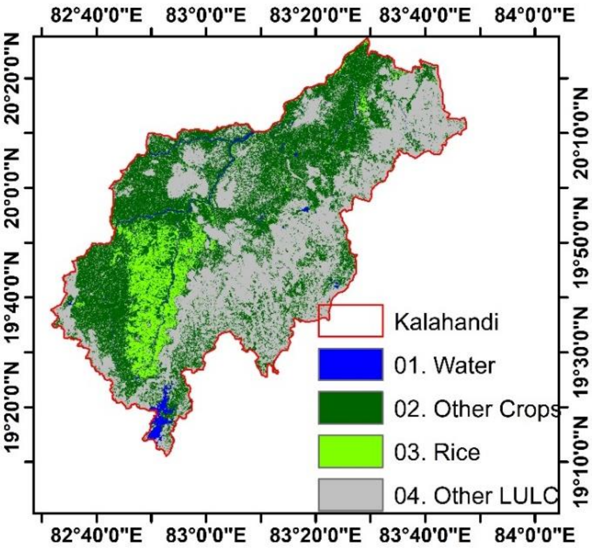

Telangana

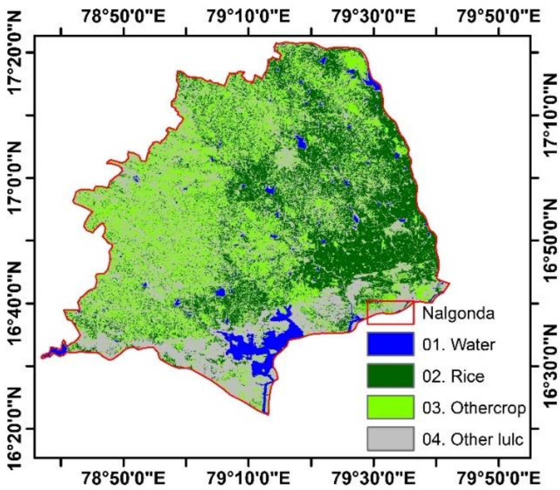

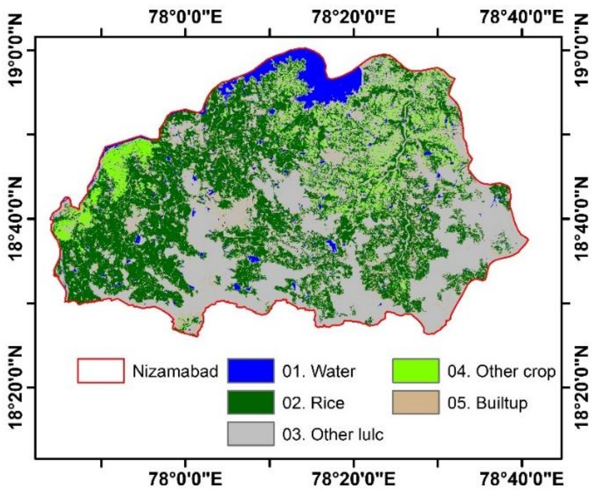

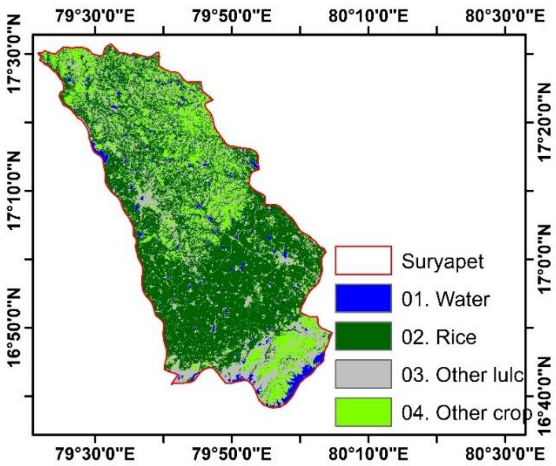

Uttar Pradesh

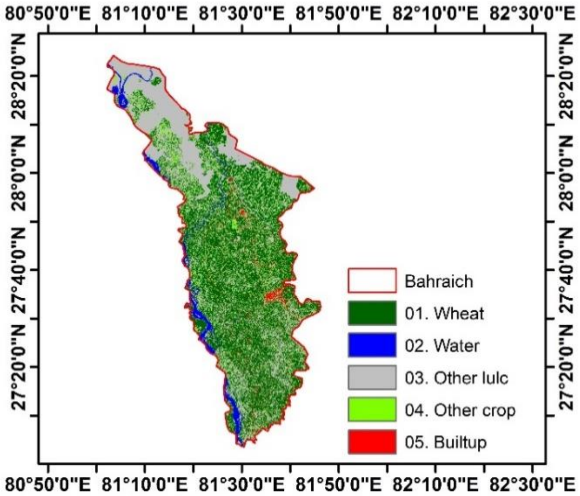

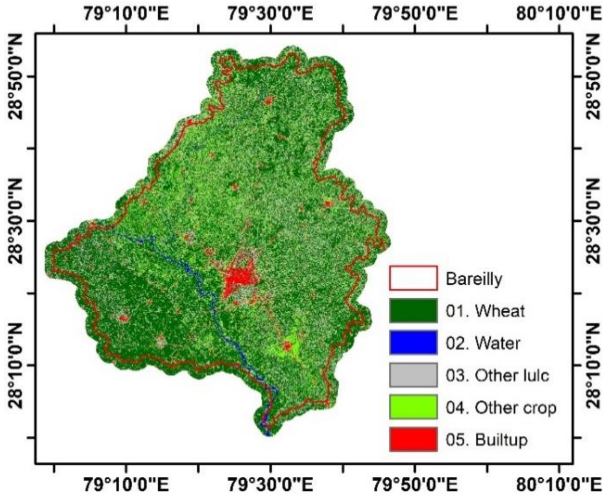

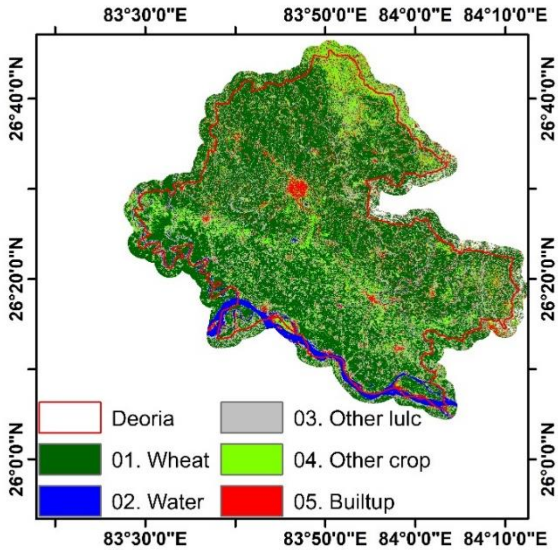

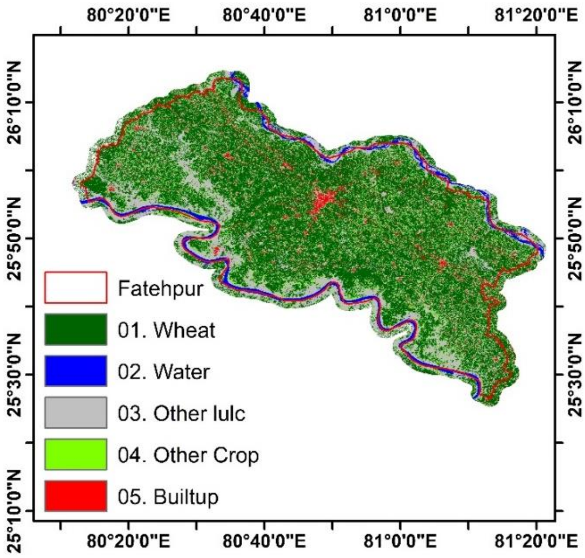

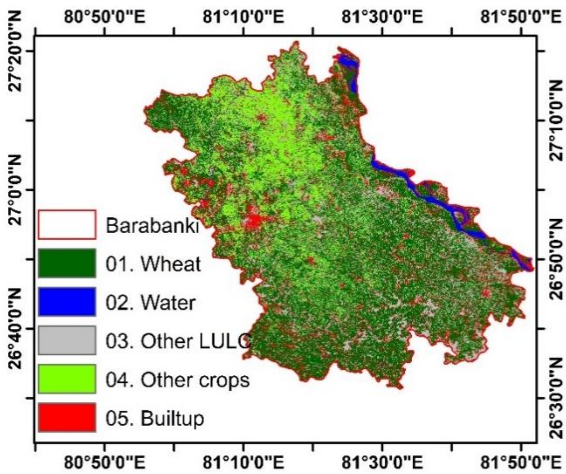

Uttarakhand

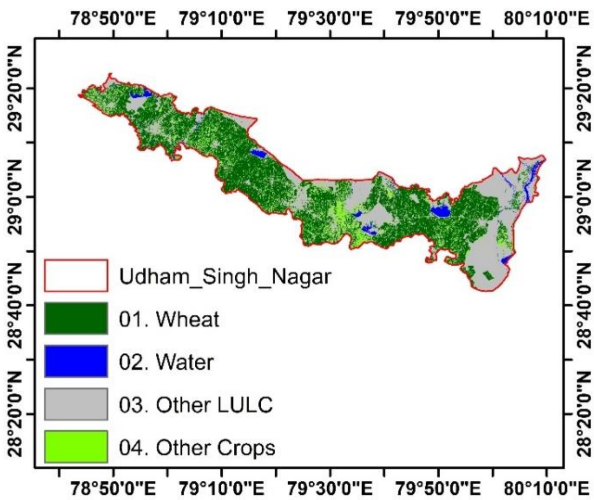

Fig 2: Crop Classification maps for study districts

CCE's Data Optimisation:

The optimisation of CCE's were carried out using following methodology (Fig.3). The process begin with collection of sentinel 2 NDVI Maximum data (available), climate data and soil map.

The NDVI data with crop mask and respective climate and soil data were combined into homogenous stratum and collected random points using stratified sampling. By multiple regression techniques, the number of samples were reduced into half of random samples.

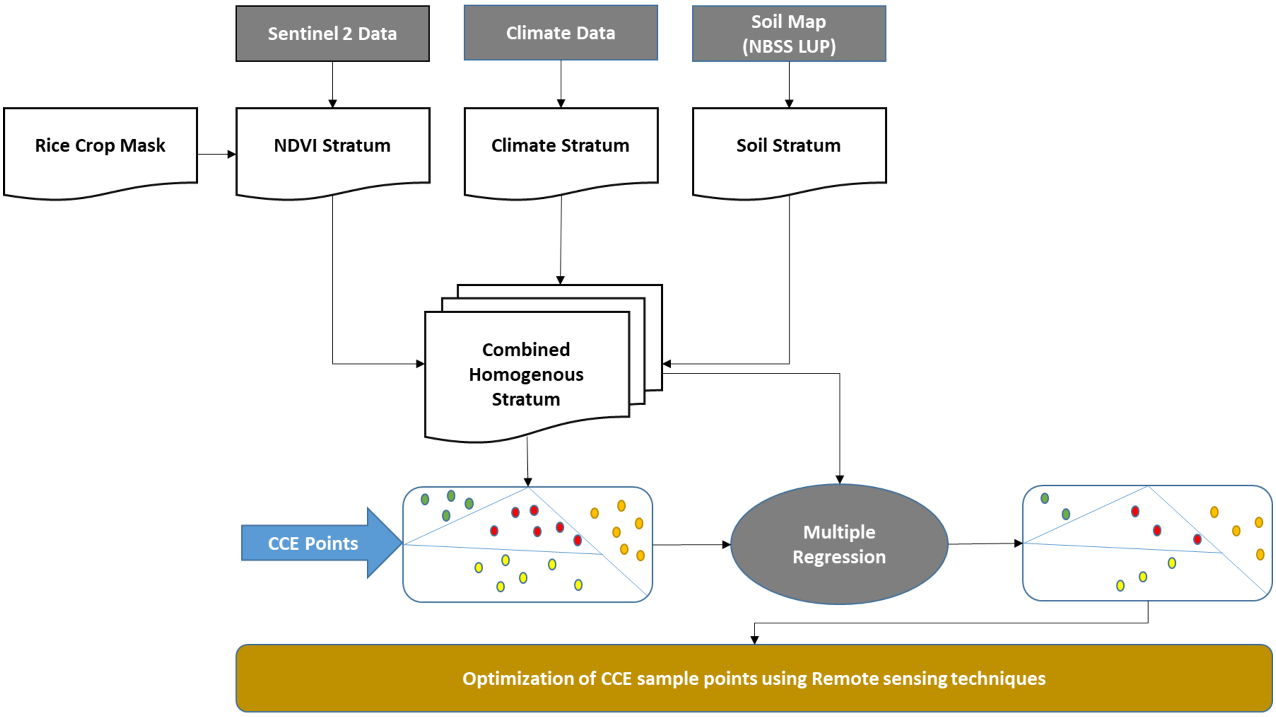

Fig.3 : Optimisation of Crop Cutting Experiments using remote sensing techniques

Using above optimization, we instructed our field staff to collect the possible samples.

CCE's Data Collection:

Based on spatial map of Crop extent, optimization and Leaf Area Index (LAI) of rice and wheat in their respective areas, the selection of CCE's were shortlisted. LAI indirectly shows the health of the crop, which helps in locating the good crop fields as well as adverse fields for collection of CCE's.

The CCE's was carried out by selecting 5m X 5m plot of field, manually harvested and weighted as shown in following images.

The total number of 160 samples were collected for each district (Annexure 1).

Locations of CCE's collected (Fig 4)

Andhra Pradesh

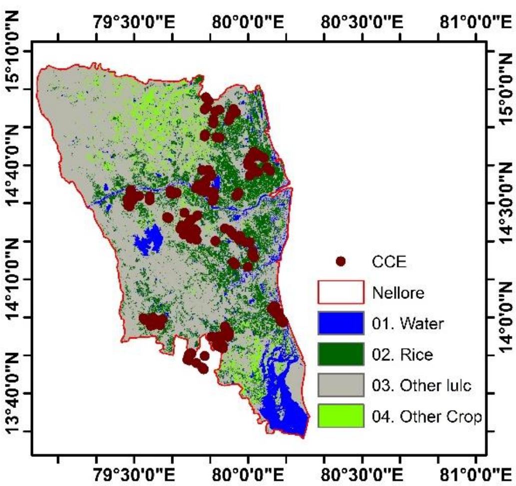

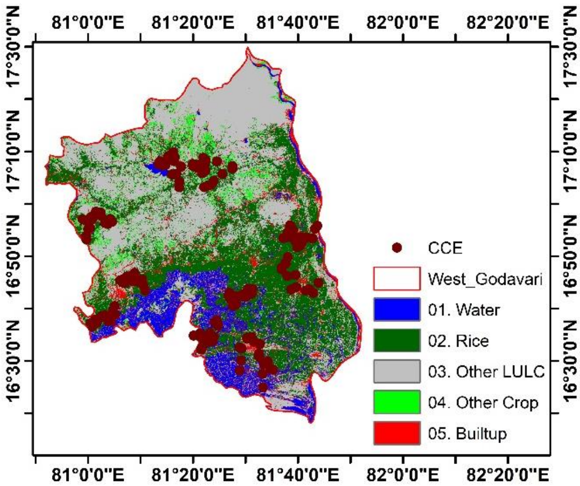

Gujarat

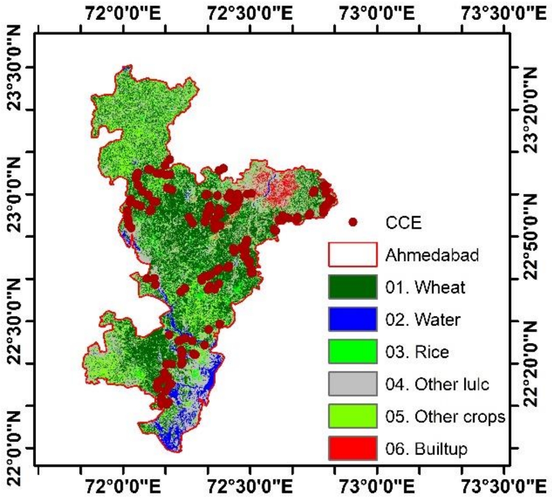

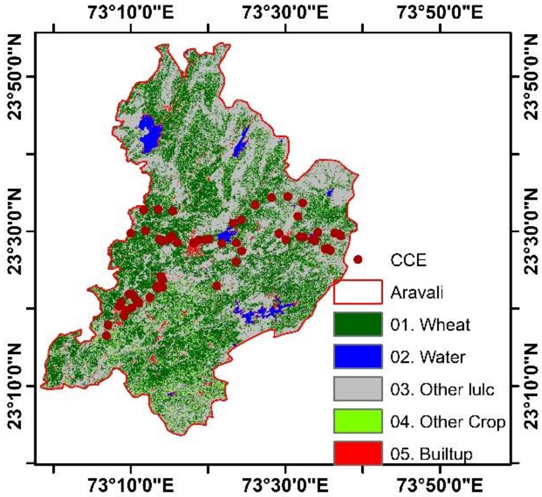

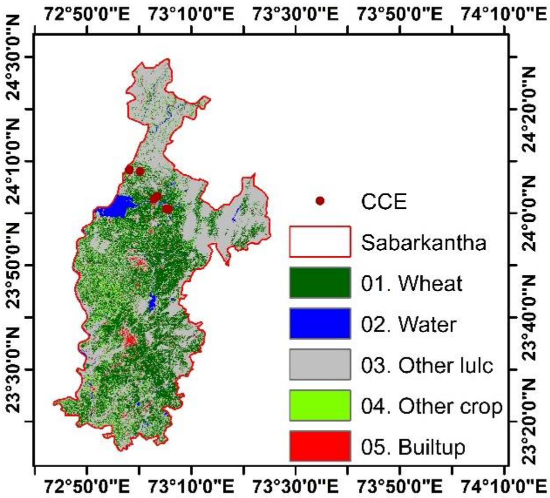

Madhya Pradesh

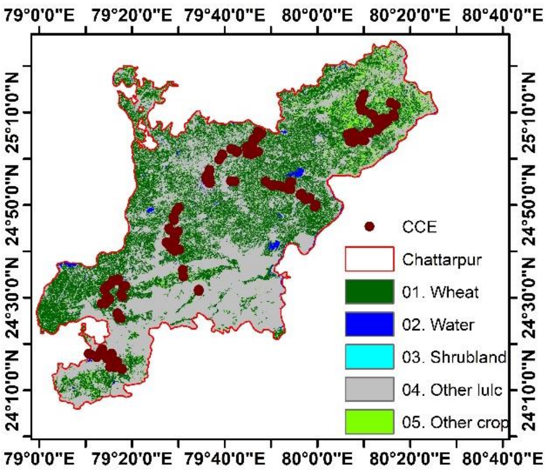

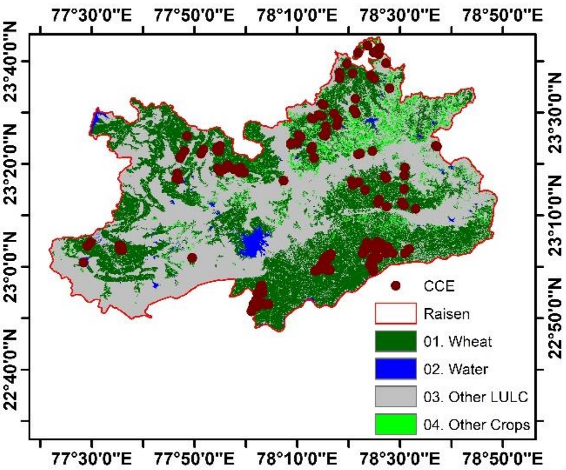

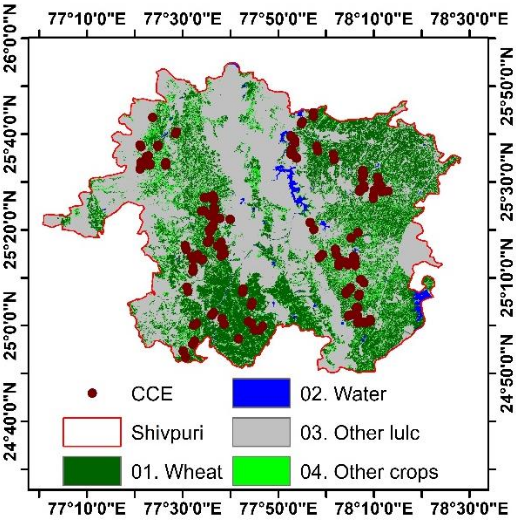
77°10'0"E
77°30'0"E
77°50'0"E
78°10'0"E
78°30'0"E
26°0'0"N
25°40'0"N
25°20'0"N
25°0'0"N
24°40'0"N
25°50'0"N
25°30'0"N
25°10'0"N
24°50'0"N
CCE
Shivpuri
01. Wheat
02. Water
03. Other lulc
04. Other crops

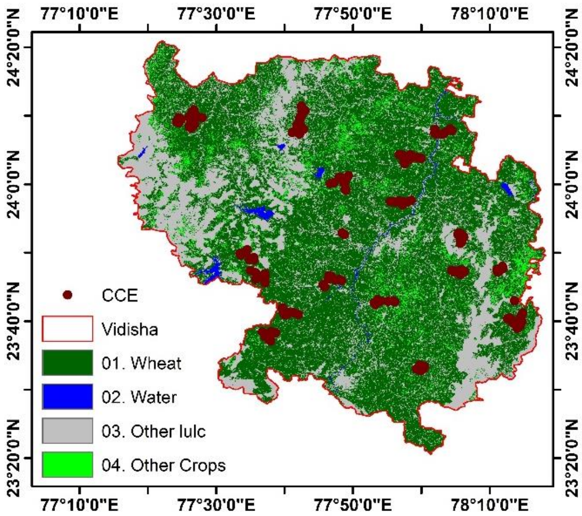
77°10'0"E
77°30'0"E
77°50'0"E
78°10'0"E
24°20'0"N
24°0'0"N
23°40'0"N
23°20'0"N
CCE
Vidisha
01. Wheat
02. Water
03. Other lulc
04. Other Crops

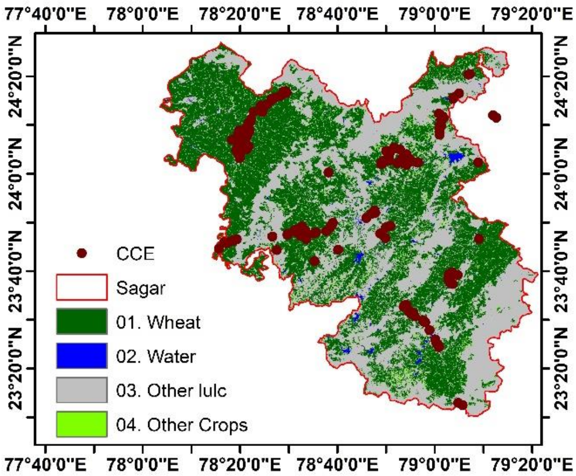
77°40'0"E
78°0'0"E
78°20'0"E
78°40'0"E
79°0'0"E
79°20'0"E
24°20'0"N
24°0'0"N
23°40'0"N
23°20'0"N
CCE
Sagar
01. Wheat
02. Water
03. Other lulc
04. Other Crops

Telangana

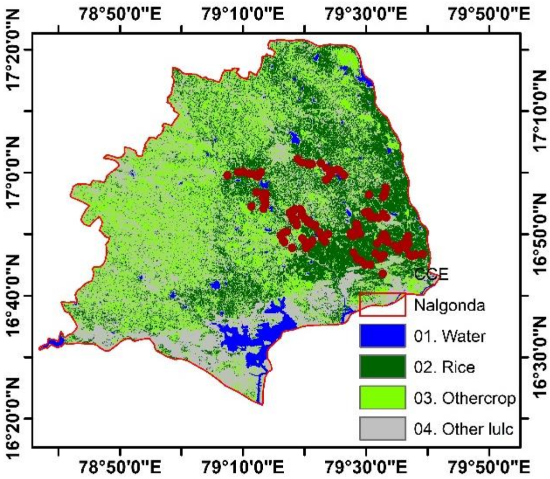

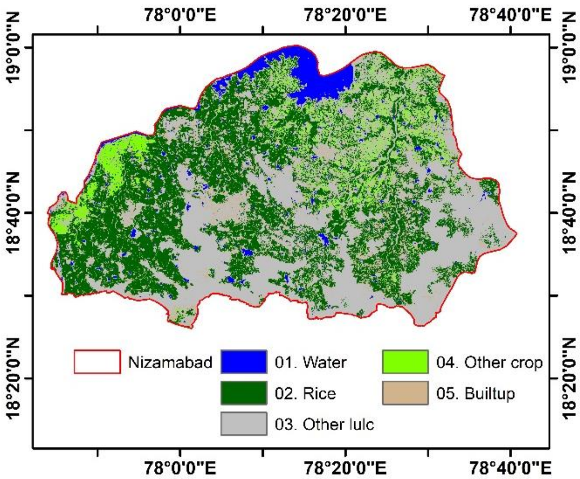

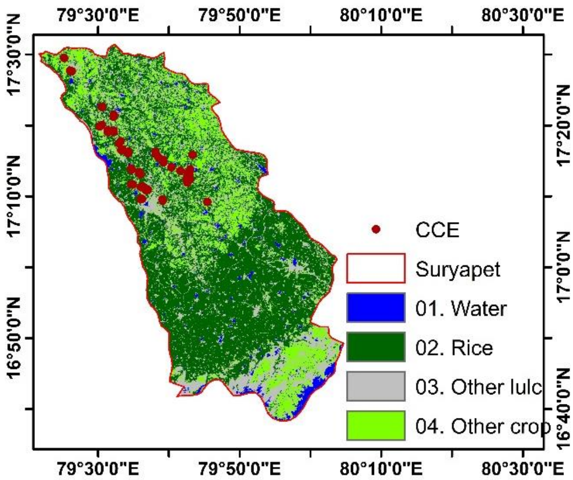

Uttar Pradesh

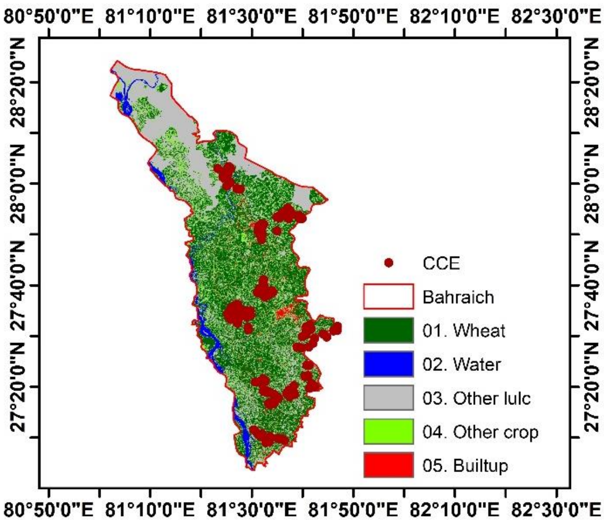

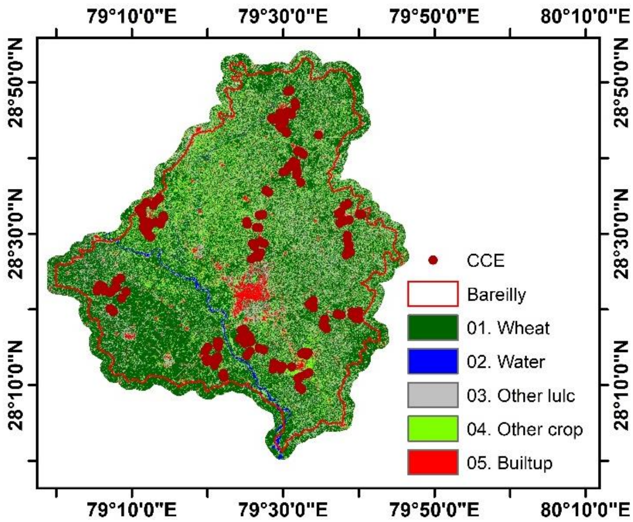

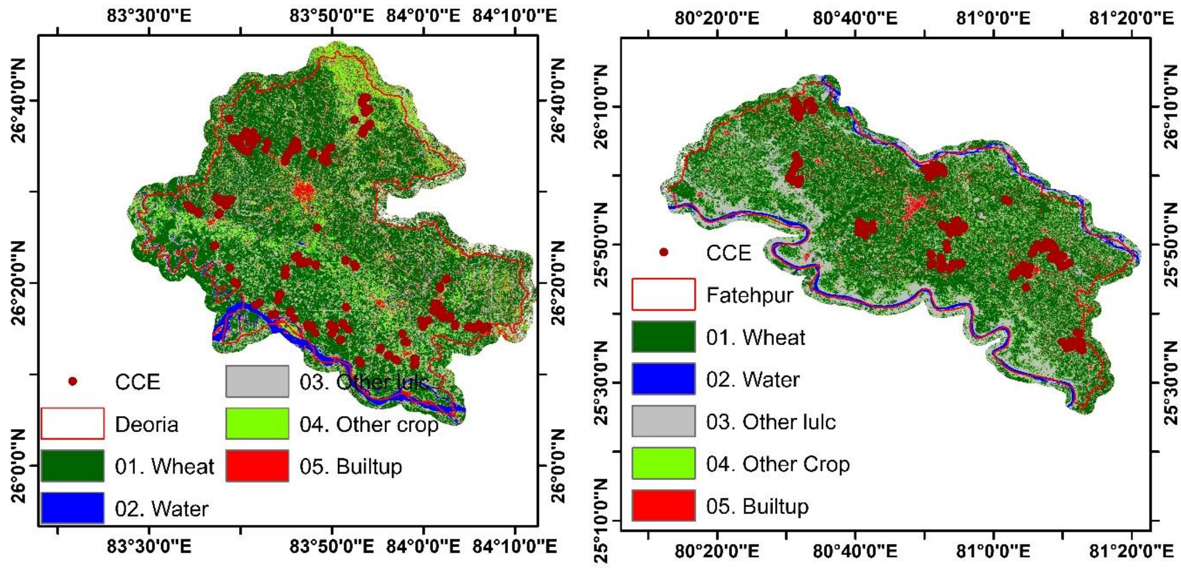

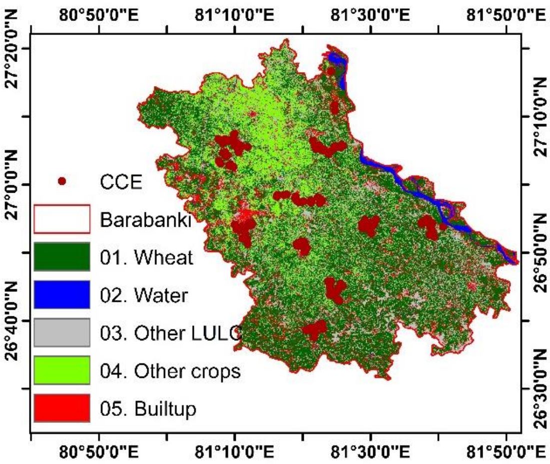

Uttarakhand

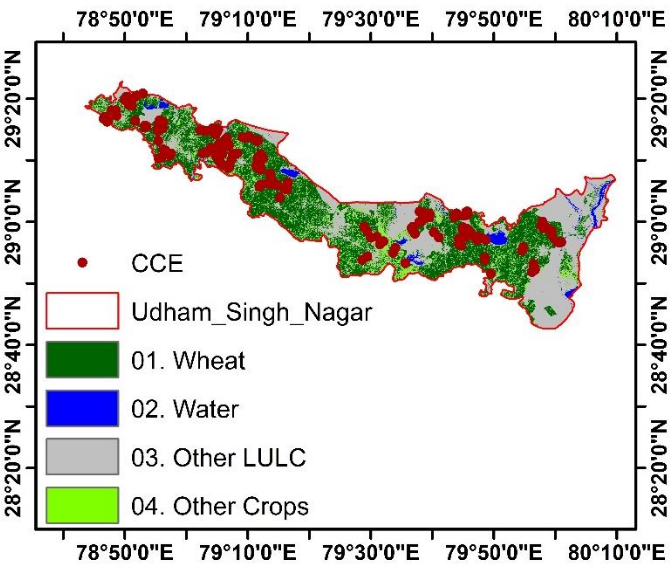

Fig 4: CCE's distribution across study districts

5. Leaf Area Index

This study used MODIS derived LAI and also sentinel -2 derived LAI index.

- Based on the fact that the spectral response of leaves is unique compared to that of other parts of the plant.
- Vegetation indices – NDVI, EVI, SAVI, etc. – have shown high positive correlation to LAI.
- With a limited field data consisting of LAI values at few locations, regression equations can be arrived at, relating LAI to spectral vegetation indices.
- METRIC (Measuring Evapotranspiration at high Resolution with Internalized Calibration) model has developed a relation between LAI and Sentinel 2-derived Soil Adjusted Vegetation Index (SAVI). According to METRIC model,

$$LAI = \frac{-\ln\left(\frac{0.69 - SAVI}{0.59}\right)}{0.91}$$

For Landsat-8 images used in this study, SAVI is computed from the formula:

$$SAVI = \frac{(1 + L)\ (B8 - B4)}{L + B8 + B4}$$

Where L is a soil factor, taken to be 0.1, B8 in the spectral reflectance in band 8 (Near Infrared) and B4 is the spectral reflectance in band 4 (Red).

Due to Coarse resolution of MODIS, the study uses LAI derived from Sentinel 2. Compared both values and used the optimised values.

LAI values were extracted for every CCE location and validated against the DSSAT crop model LAI

Integration of remote sensing LAI products with crop simulation models for better crop yield estimation

1. Introduction

Timely and accurate prediction of crop yield is important for agricultural land management and policy making. Several studies have demonstrated the utilization of satellite data in crop yield estimation. However, majority of studies used methods of empirical nature and they work only for specific locations, crops, cultivars and for a particular crop growth stage. Cropping system models and remote sensing tools are two different methodologies often used to answer some of the agronomic questions at various levels such as field and regional scales. Several researchers used these technologies independently however information derived from remote sensing is used to update cropping systems model simulations in recent times as both these technologies are complementary.

Keeping in view the complimentary nature of these technologies several researchers started integration of remote sensing data with crop growth simulation models found to be a promising option for crop growth monitoring and yield estimation. However, each technology has its own advantages limitations. For example use of remote sensing as a temporal crop analysis tool is limited due to availability of cloud free time-series remote sensing data and difficulties in accurate LAI estimation from remotely sensed data.

Similarly cropping systems models are often limited by data availability such as information on cultivar, management, soil, and meteorological inputs for spatial simulations. Uncertainties associated with spatial simulations can be reduced by periodically readjusting the simulation using spatial information from remote sensing images.

Several remote sensing data assimilation methods at various complexity levels were tried mostly either by directly using remote sensing data in the simulation models, updating the state variables or re parameterization of the model using remote sensing data in recent years.

In this study, we used the technique of re- parameterization of crop simulation models based on the several iterations using remote sensing input such as leaf area index(LAI) as it is supposed to be the highest degree of integration. The essence of the data assimilation approach is to improve the initial parameterization of the crop growth model and augment simulation with the use of remotely sensed observations.

2. Methodology

The methodology **(Fig 5)** includes crop model data mainly soil, weather and crop management data and its integration with remote sensing data.

2.1.Data collection

Crop Cutting Experiments (CCE) is an assessment method employed by governments to estimate the crop yield in the region given cultivation cycle. The traditional method of CCE is based on the yield component method where sample locations are selected based on a random sampling of the total area under study. In the current analysis, we identified few mandals in study districts in 25 districts of eight states viz. Andhra Pradesh, Gujarat, Karnataka, Madhya Pradesh, Odisha, Telangana, Uttar Pradesh and Uttarakhand, to test the methodology. Data assimilation from remote sensing products such as leaf are index (LAI) in to cropping system models to predict crop yield in CCE sites. We have collected GPS location, date of sowing, irrigated vs. rainfed and other management details from CCE location if available.

2.2.Soil data

Biophysical crop simulation models normally require profile-wise soil data. For each CCE location, soil inputs to the model were obtained from a set of soil profile data available from ICRISAT data repository and NBSSLUP data bases. We also used certain parameters in soil as free variable. Soil physical and chemical properties such as texture, hydraulic parameters, bulk density, organic matter and available N were extracted for each location based on the available soil profile data. Additional soil parameters such as soil albedo, drainage constant, and runoff curve number were estimated based on soil texture and converted using the generic soil database available in the DSSAT-models.

2.3.Weather data

The weather data such as daily maximum temperature, minimum temperature, rainfall and solar radiation data was collected from Automatic Weather Stations (AWS) stations of respective state authorities. If AWS data not available, NASA power data was used for analysis.

2.4.The Cropping System Model

The Cropping System Model (CSM)–Crop Environment Resource Synthesis (CERES)–Rice and wheat crop growth model as provided in the Decision Support System for Agro technology Transfer (DSSAT) were used for yield simulations. Crop models require various input data such as crop characteristics, soil condition, management practice and daily weather information were prepared in advance. Using these input data, daily crop biophysical information (e.g. LAI) was generated by the crop growth model. The simulated LAI were compared with the corresponding Sentinel 2 and MODIS LAI products, and residuals between the simulated and Sentinel 2 LAI were minimized by adjusting the free input parameters, finally with the optimized set of input parameters, the model was executed to update the crop yield prediction.

The optimization process starts from an initial parameterization and adjusts the free parameters in order that the model given LAI with simulation is in agreement with the Sentinel 2 Observations. The simulated LAI values depend on the values of the free variables (e.g. planting date, nitrogen dose, soil profile parameters) that are estimated by minimizing the cost function as shown below.

$$= \frac{1}{m}\sum_{i=1}^{m} \text{abs}\left[(\text{LAI})_S(t_i) - (\text{LAI})_M(t_i)\right] / (\text{LAI})_M(t_i) \quad \text{--- Equation -1}$$

Where LAIS (ti), LAIM (ti) are the simulated and measured LAI at time t_i, respectively.

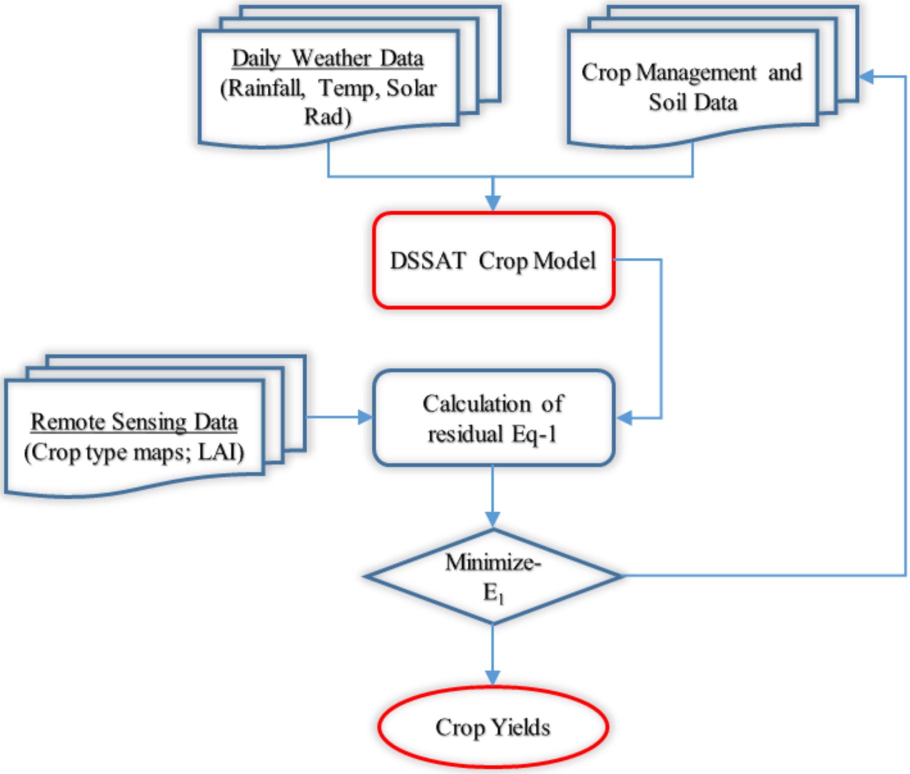

Fig 5. General methodology of the data assimilation approach integrating remote sensing data with crop growth models for crop yield estimation

2.5. Assimilation of Remote Sensing Data into Crop Growth Model for Yield Estimation

Remote sensing data assimilation methods with various levels of complexity have been tried, either by directly using remote sensing satellite data in simulation models (Doraiswamy, Moulin, Cook, & Stern, 2003; Olioso et al., 2005), by updating state variables or by re-parameterization of the model using remote sensing satellite data (Fang, Liang, & Hoogenboom, 2011; Jin et al., 2017)., we used the technique of re-parameterization of crop simulation models through several iterations using remotely sensed LAI estimates; this technique is supposed to best integrate crop growth conditions. The data assimilation approach helps with initializing parameters of the crop growth model and improve simulations with the help of remotely sensed satellite observations. The optimization process starts with initial model parameterization by adjusting the free parameters so that the model-simulated LAI is in agreement with the Sentinel-2 LAI observations (Eq. 1). The simulated LAI values depend on the values of the free variables (e.g., planting date, nitrogen dose, soil profile parameters) that are generated by minimizing the value of the following cost function. The remote sensing LAI data were collected for six times during the crop growth period.

$$= \frac{1}{m}\sum_{i=1}^{m} \mathrm{abs}\left[(\mathrm{LAI})_{\mathrm{S}}(t_i) - (\mathrm{LAI})_{\mathrm{M}}(t_i)\right] / (\mathrm{LAI})_{\mathrm{M}}(t_i) \quad \text{--- Equation -1}$$

Where LAIS (ti), LAIM (ti) are the simulated and measured LAI at time t_i, respectively.

Using a cost function measuring the distance between the simulated state variables and observed ones, the method employed automatically adjusts the set of model input parameters until the difference between the Sentinel 2 LAI and the crop model-simulated LAI is minimized. Finally, using this optimization algorithm, crop yields were predicted at each CCE location by obtaining a new set of parameters or initial values and allowing a simulation that resembles better observations. The technique we used was a frequently applied re-calibration methodology that enabled us to estimate the yields of rice and wheat successfully and compare them with observed yields with significant accuracy at each CCE location. The data assimilation approach proved to be reliable and shows great potential in providing yield prediction data at the village level. In this study, since LAI is the only link between the crop growth model and remotely sensed data, the accuracy of the model and final predictions with optimized datasets depends on the quality of remotely sensed LAI data

2.6. Calibration of DSSAT and Validation of yield data at GP level

DSSAT crop models require genetic coefficients, which are cultivar specific for describing processes related to growth and development and grain production. These coefficients allow the model to simulate performance of diverse genotypes under different soil, weather and management conditions. The model was calibrated using field measured values of weather parameters, crop management and soil properties during the cropping season. In our previous studies as a part of Agricultural Model Intercomparision and Improvement Project (AgMIP) phase I & II, we have calibrated CERES-rice and wheat model for various cultivars of different duration

As, the model was run at CCE plot level, the observed yield of every CCE collected was validated against the crop model yield generated by re-parameterization of the model free variables using remote sensing LAI data. The rice and wheat yields depends mainly on crop management practices followed mainly nitrogen amount and time of application, irrigation application rates, cultivar duration etc., The village mean yield was calculated with collected CCE yield and corresponding simulated yields.

As some times models may underestimate LAI as seen in several published literature and hence we re-parameterized the CERES rice model variables using LAI developed from remote sensing data at regular intervals during crop growth period. However, the accuracy issues for remote sensing LAI may be possible due to due to cloud conditions and varying spectral indices. Further improvements of the Sentinel-derived LAI and vegetation index products are necessary, especially during the beginning of the growing season and continued data during the crop growth period. There is also an immediate need to further invest in studying relationship between remote sensing derived LAI product and field LAI observations across locations to understand the accuracy of remote sensing LAI predictions

Future Improvements:

- Improvements in LAI predictions
- Use of remote sensing derived dry matter production and other indices in addition to LAI to re-parameterization of model free variables for improving accuracy of predictions
- Exploring the possibility of establishing a good network of AWS stations for accurate location specific daily weather data for better prediction of crop yields

3.0. Study sites –Results

3.1 Nellore

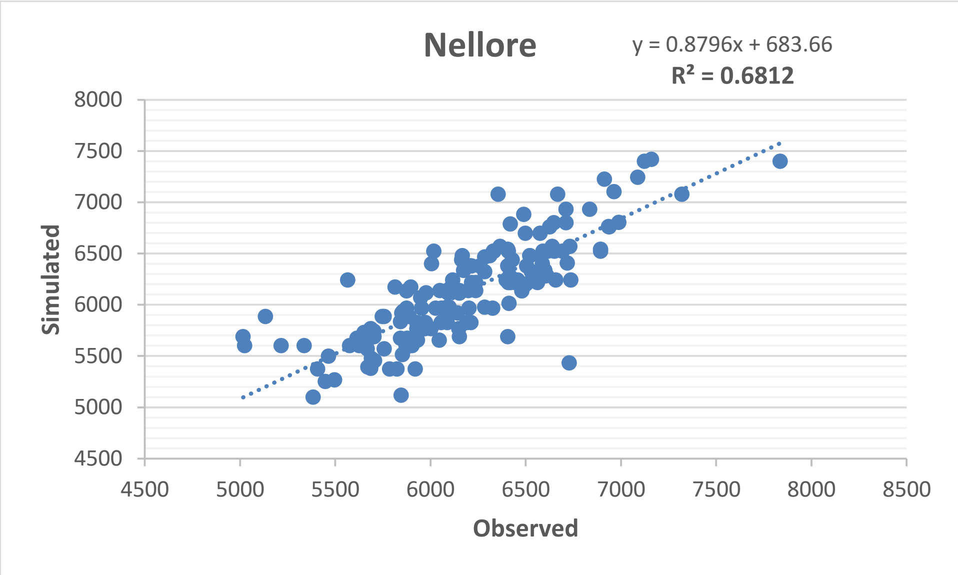

R2	0.68117836	
RMSE	286.367928	
IoA	0.71213137	
T-test	0.25059436	insignificant

3.2 West Godavari

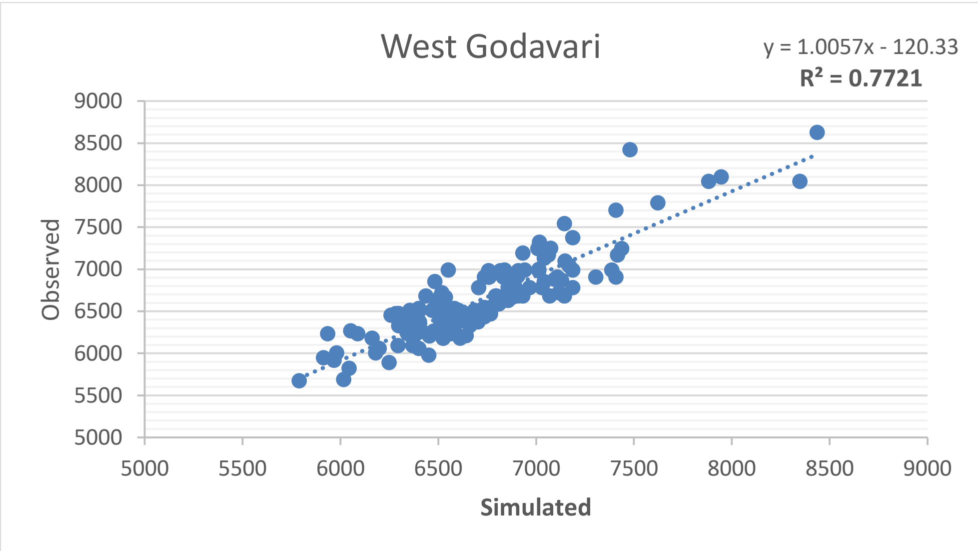

R2	0.77213827	
RMSE	242.25725	
IoA	0.6931874	
T-test	0.11313948	insignificant

3.3 Shivpuri

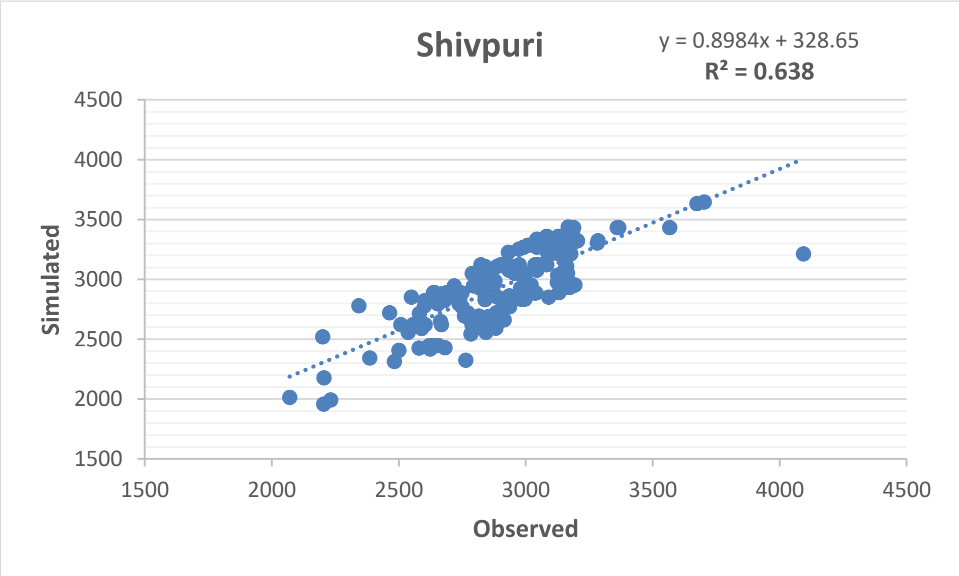

R2	0.63803941	
RMSE	192.255651	
IoA	0.68285436	
T-test	0.29679147	insignificant

3.4 Chattarpur

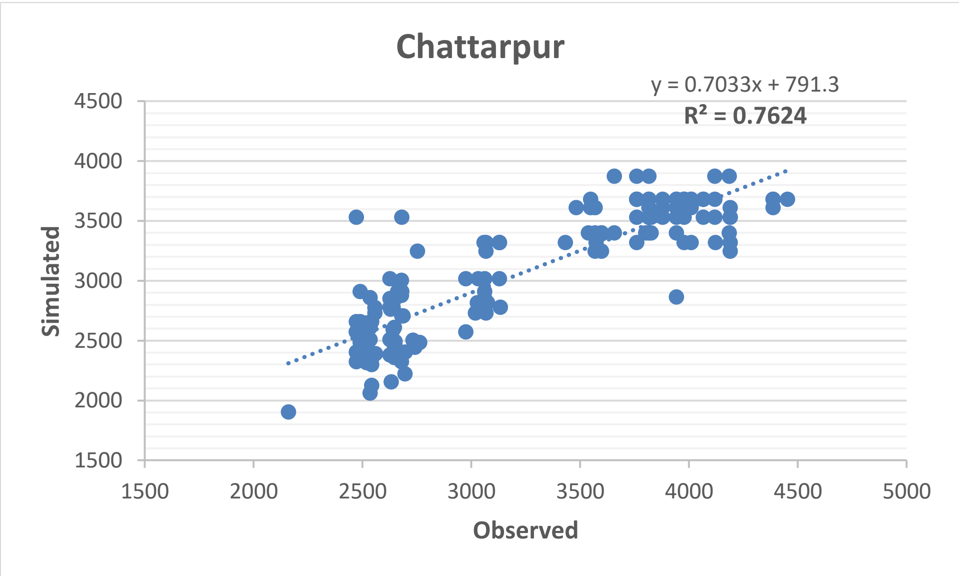

R2	0.76241427	
RMSE	353.902662	
IoA	0.76840674	
T-test	0.01182702	Significant

3.5 Raisen

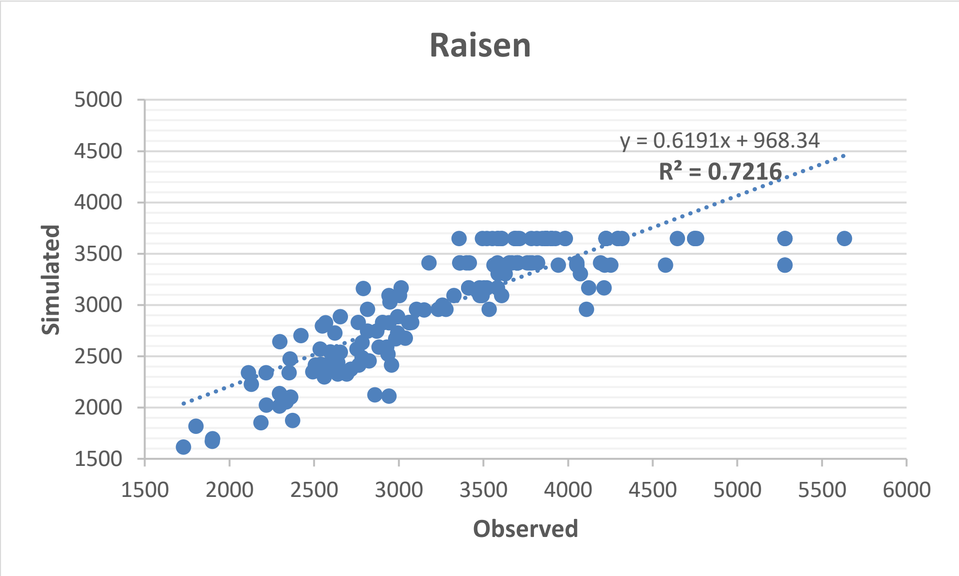

R2	0.721560238	
RMSE	474.5357838	
IoA	0.785992093	
T-test	3.84581E-05	Significant

3.6 Sagar

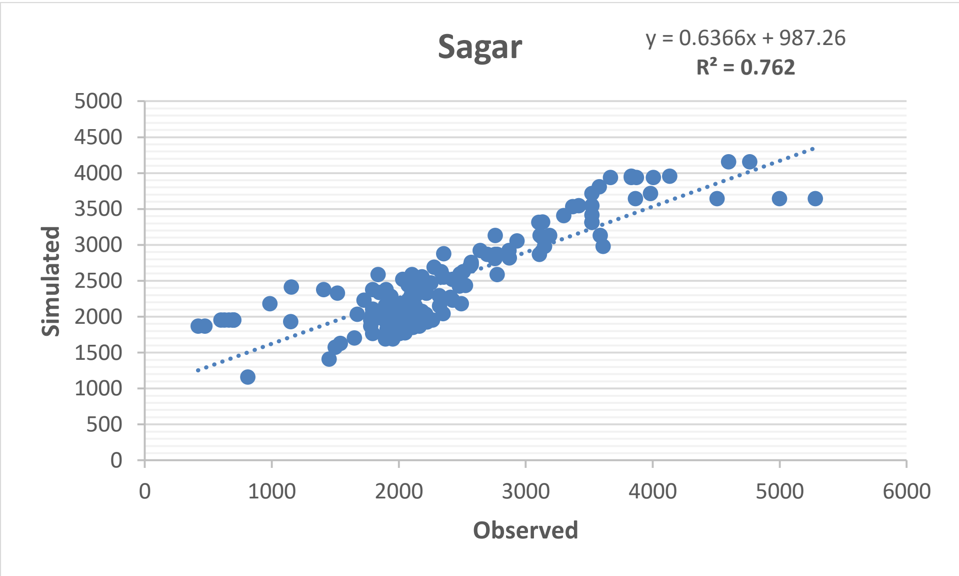

R2	0.76195482	
RMSE	465.118228	
IoA	0.80473189	
T-test	0.08585808	insignificant

3.7 Vidisha

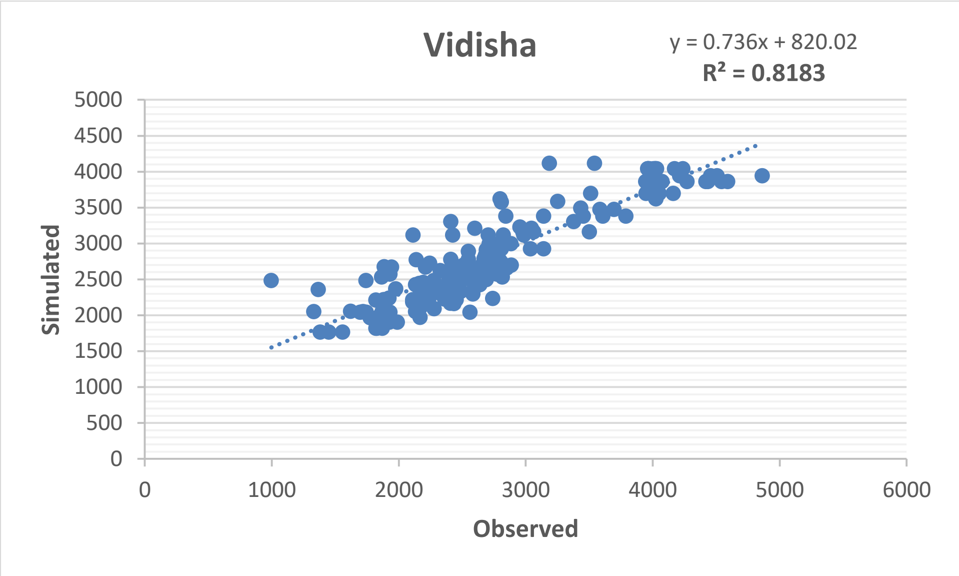

R2	0.81832035
RMSE	369.624642
IoA	0.78767549
T-test	0.28005764 insignificant

3.8 Bareilly

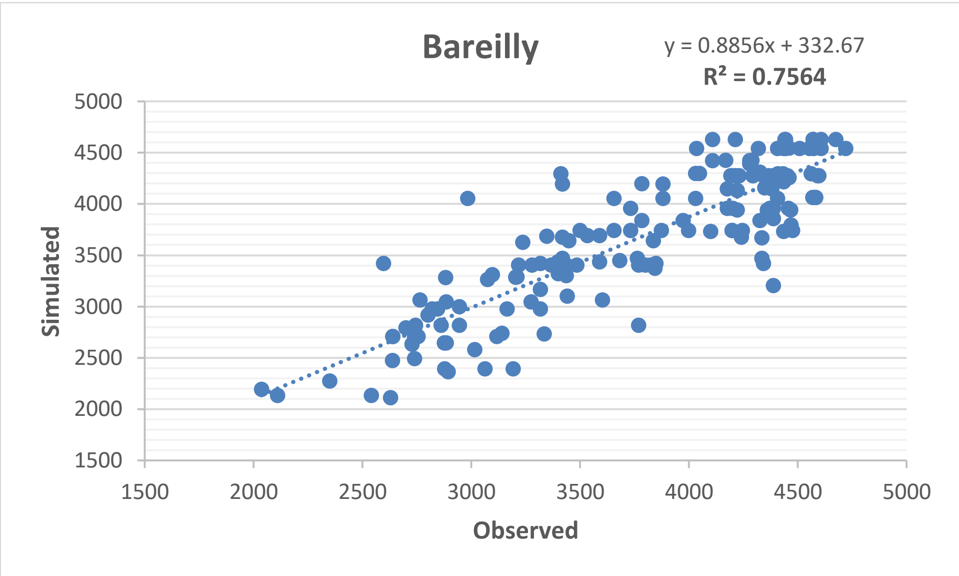

R2	0.75639265
RMSE	355.836826
IoA	0.72969145
T-test	0.17154472 insignificant

3.9 Barabanki

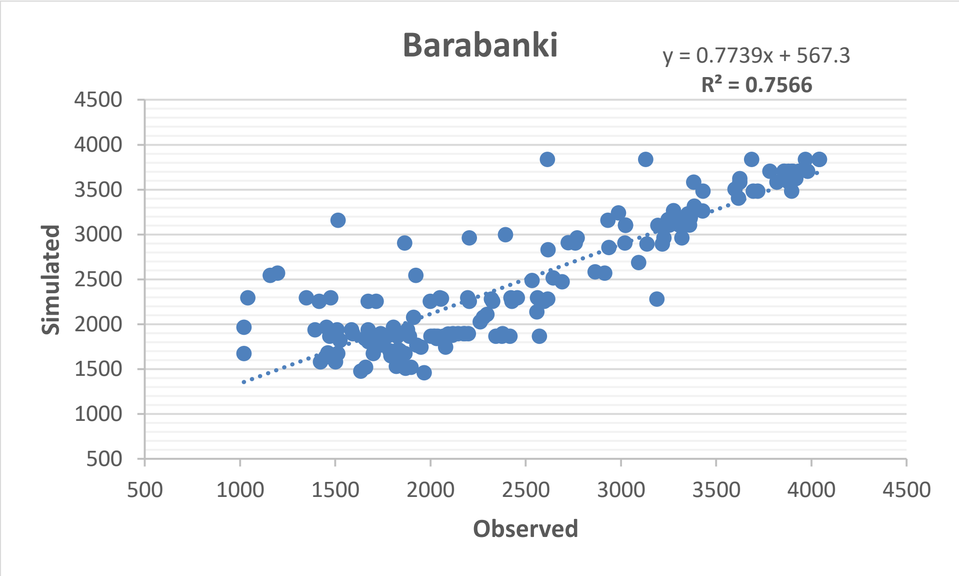

R2	0.75659806
RMSE	501.327643
IoA	0.76022787
T-test	0.96705721 insignificant

3.10 Bahraich

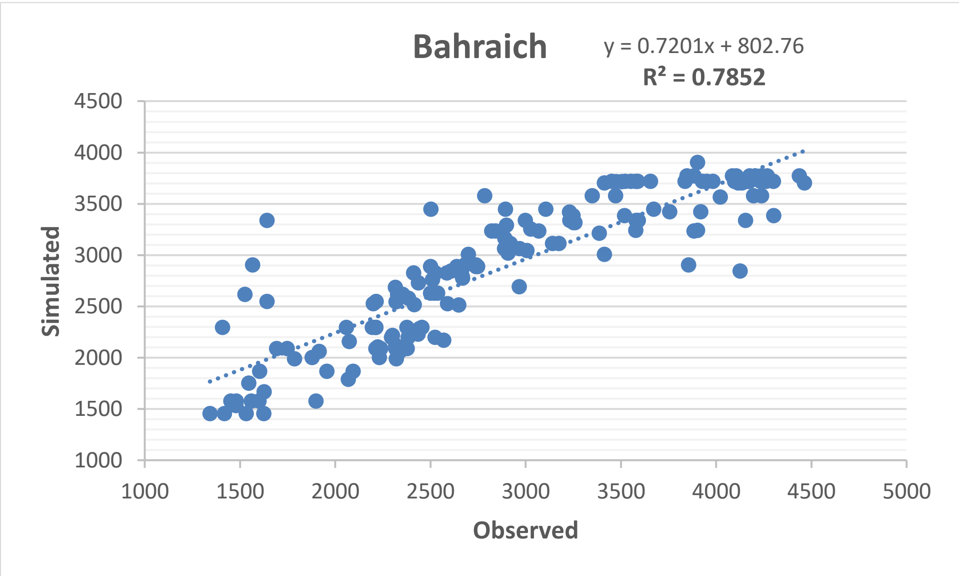

R2	0.785206
RMSE	404.777971
IoA	0.78937681
T-test	0.90317337 insignificant

3.11 Fatehpur

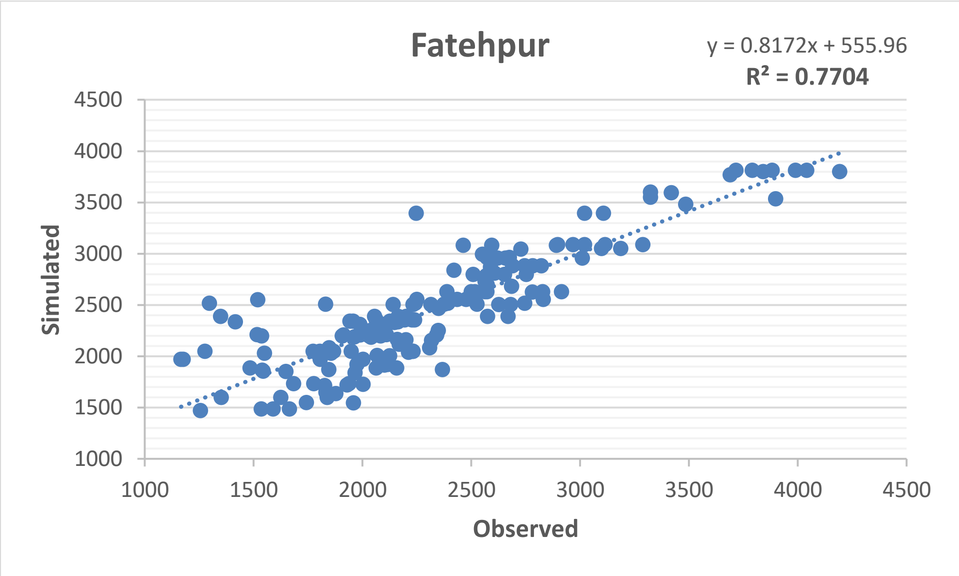

R2	0.77041913	
RMSE	324.74852	
IoA	0.74530749	
T-test	0.05480408	insignificant

3.12 Deoria

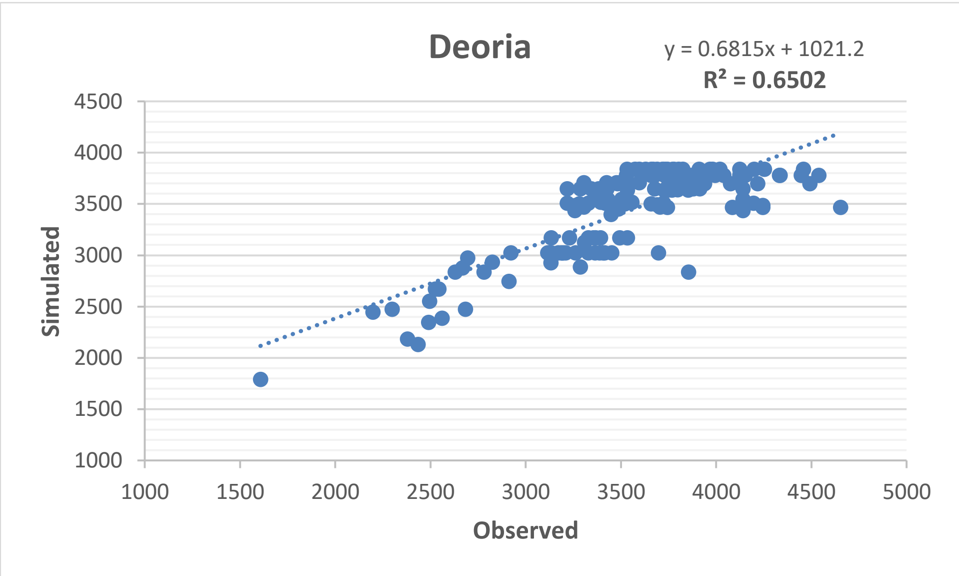

R2	0.65019329	
RMSE	314.610411	
IoA	0.76302657	
T-test	0.02680672	Significant

3.13 Udham Singh Nagar

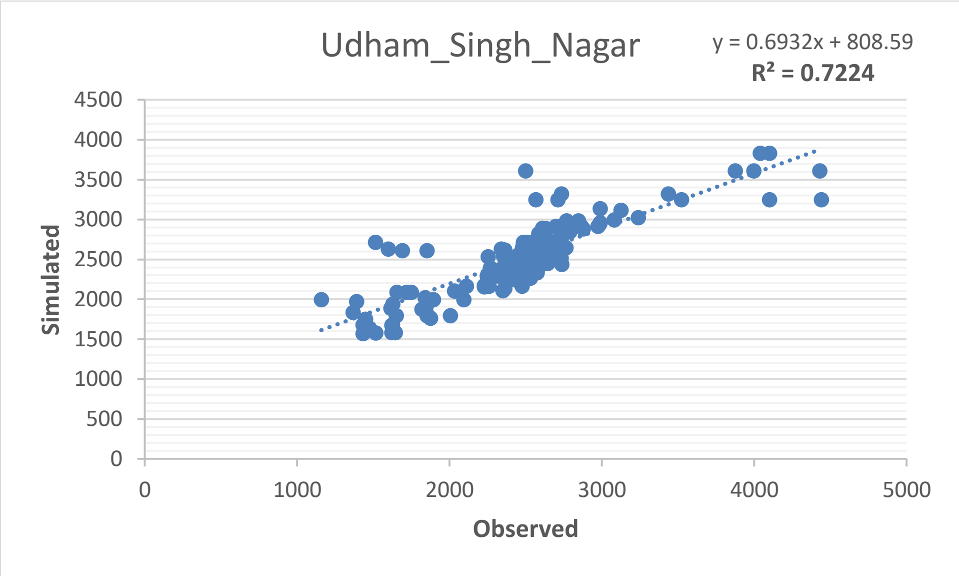

R2	0.72235465	
RMSE	293.691582	
IoA	0.78404631	
T-test	0.3111512	insignificant

3.14 Ahmedabad

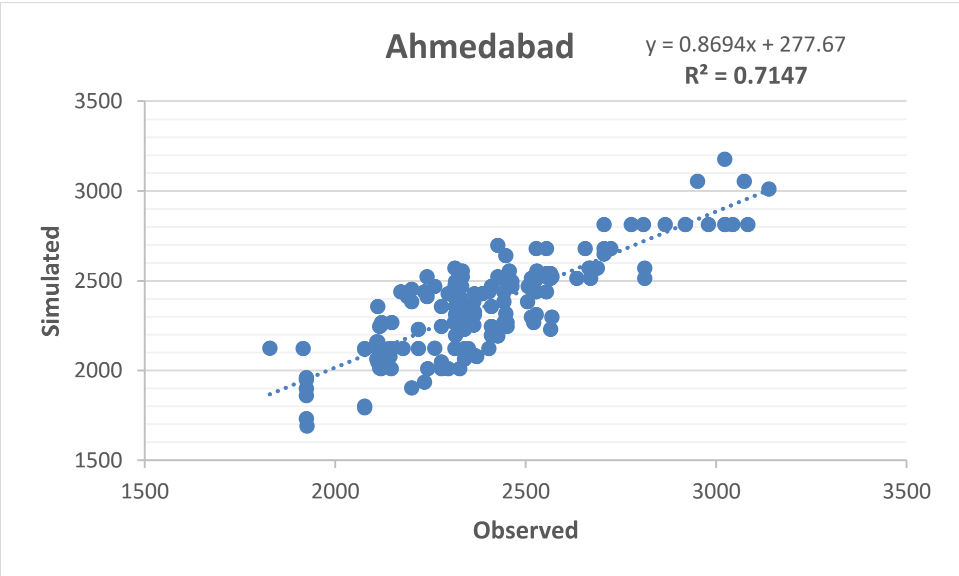

R2	0.71467418	
RMSE	151.772712	
IoA	0.72481833	
T-test	0.24260612	insignificant

3.15 Nalgonda

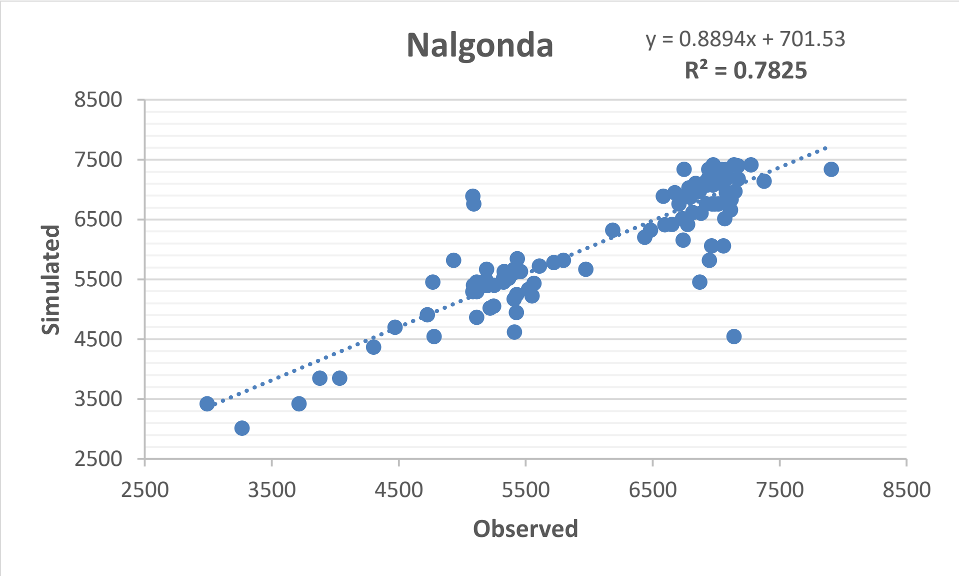

R2	0.78250336	
RMSE	489.315232	
IoA	0.74254863	
T-test	0.87548151	insignificant

3.16 Suryapet

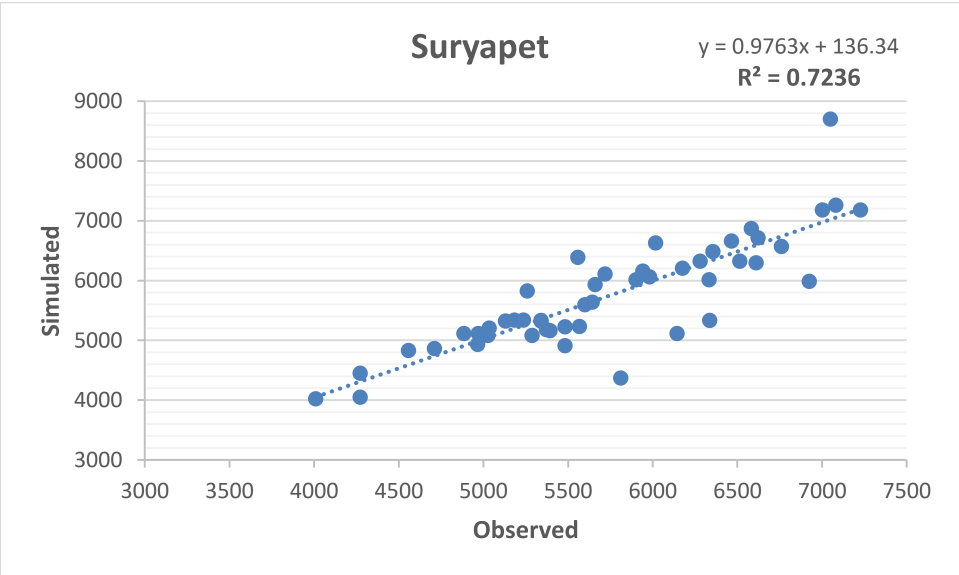

R2	0.72356923	
RMSE	472.110645	
IoA	0.69883744	
T-test	0.99920203	insignificant

3.17 Aravalli

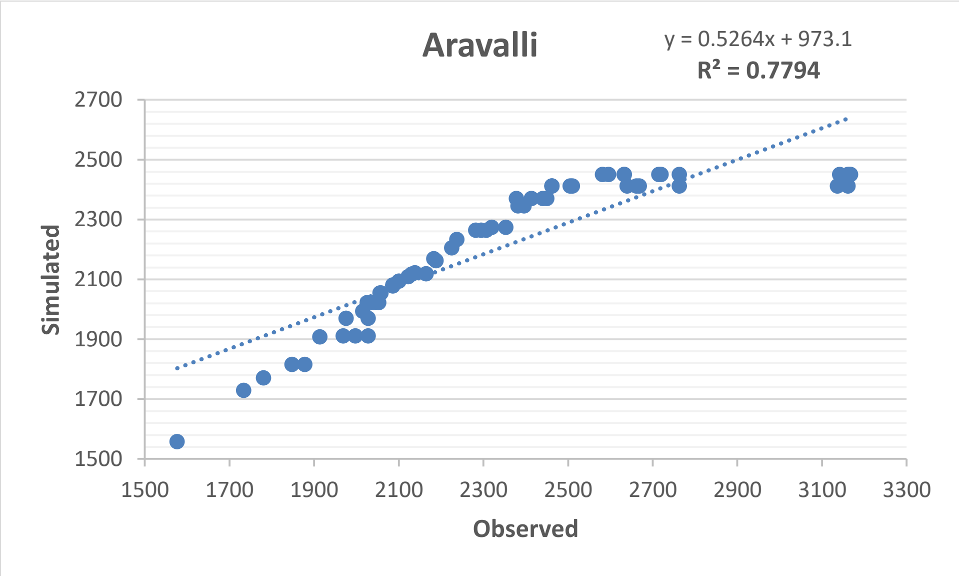

R2	0.77942159	
RMSE	252.395806	
IoA	0.8081811	
T-test	0.01855601	Significant

3.18 Nizamabad

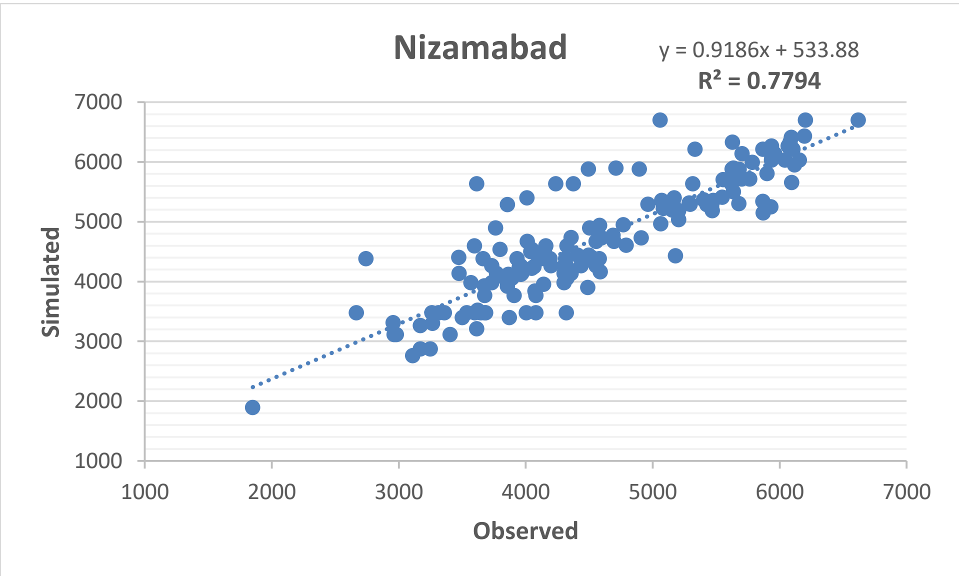

R2	0.77940507	
RMSE	498.92488	
IoA	0.72459841	
T-test	0.13847399	insignificant

3.19 Kalahandi

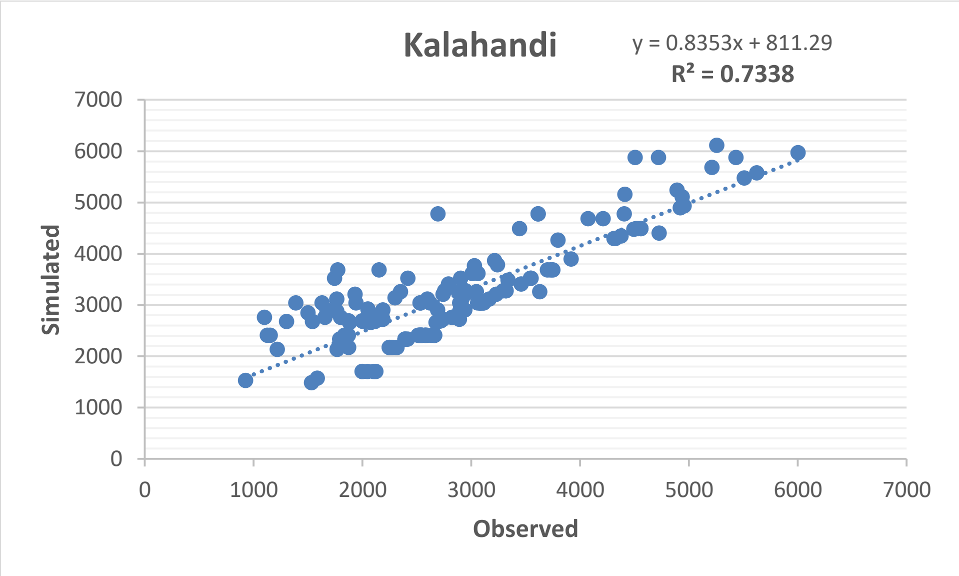

R2	0.733842799	
RMSE	645.2578191	
IoA	0.724627237	
T-test	0.003073212	Significant

3.20 Baragarh

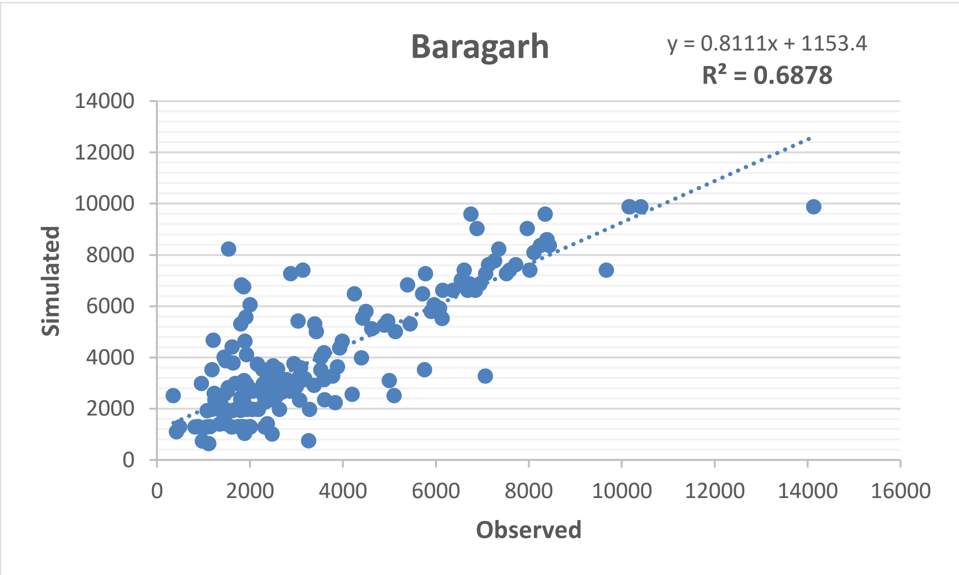

R2	0.68775755	
RMSE	1510.450046	
IoA	0.739596979	
T-test	0.081970818	insignificant

3.21 Baleshwar

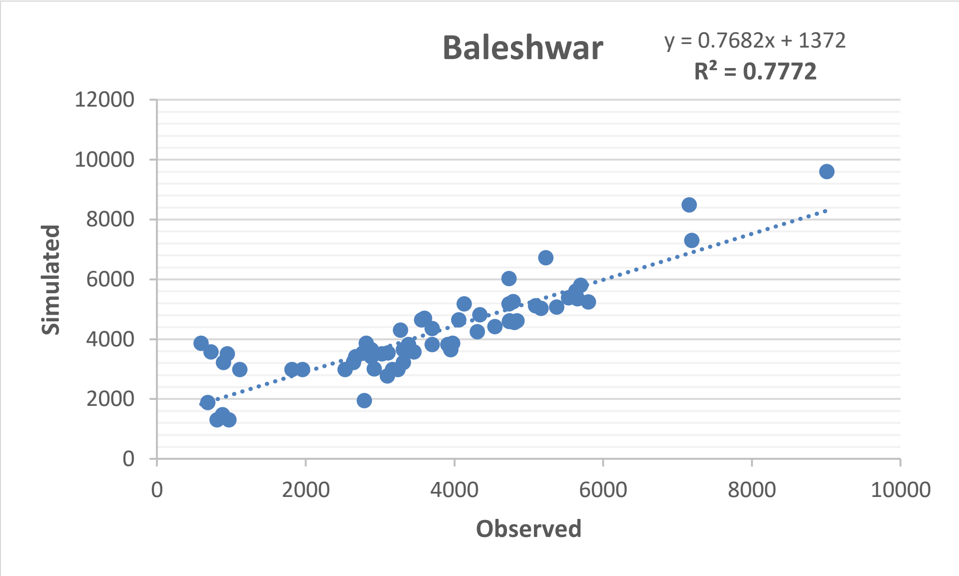

R2	0.77718502	
RMSE	969.540245	
IoA	0.75043209	
T-test	0.07655976	insignificant

4.0. Gram Panchayat level Yield Estimations

Attached as Annexures

5.0. Challenges and improvements

This study indicates the importance of LAI in the data assimilation process and that the incorporation of LAI can improve crop yield prediction. However, the following points need to be considered to further improve the yield prediction.

1. There is a need to study the relationship between remote sensing derived LAI product and final yields of various crops especially in rain-fed regions.
2. Further improvements of the Sentinel 2 -derived LAI and vegetation index products are necessary, especially during the beginning of the growing season and continuous data during the crop growth period.
3. The availability of location-specific weather data is the key for proper simulations with crop simulation models. In some states there exists a good network of AWS stations, however the majority of other locations this is major lacunae.

Annexure 1:

State	District	Crop	iCrops	Bhuvan_GT	GT_Validation	GT_Status	Classification	Accuracy(%)	CCE	CCE_Bhuvan	CCE_Status	Weather Data	Soil Data	Yield Estimation	R2	RMSE	IOA	t-test
Andhra Pradesh	**Nellore**	Rice	214	230	261	✓	✓	87.74	163	151	✓	✓	✓	✓	0.68	286	0.71	0.250
	West Godavari	Rice	209	210	233	✓	✓	89.27	164	149	✓	✓	✓	✓	0.77	242	0.69	0.113
Gujarat	**Ahmadabad**	Wheat	222	200	252	✓	✓	87.7	164	154	✓	✓	✓	✓	0.71	152	0.72	0.243
	Aravali	Wheat	179	200	137	✓	✓	86.86	60	50	✓	✓	✓	✓	0.78	252	0.81	**0.018**
	Sabarkantha	Wheat	224	180	102	✓	✓	88.24	6	6	On hold	✓	✓					
Karnataka	**Bellary**	Rice	166	200	130	✓	✓	88.46	0	0	On hold	✓	✓					
	Davangere	Rice	155	200	175	✓	✓	88	0	0	On hold	✓	✓					
	Raichur	Rice	225	200	159	✓	✓	87.42	18	18	On hold	✓	✓					
Madhya Pradesh	**Chhattarpur**	Wheat	174	167	214	✓	✓	87.38	160	163	✓	✓	✓	✓	0.76	354	0.77	**0.011**
	Raisen	Wheat	167	160	220	✓	✓	91.36	161	148	✓	✓	✓	✓	0.72	512	0.77	**0.000**
	Sagar	Wheat	179	150	187	✓	✓	88.24	161	154	✓	✓	✓	✓	0.76	465	0.80	**0.080**
	Shivpuri	Wheat	155	150	195	✓	✓	88.21	161	136	✓	✓	✓	✓	0.64	192	0.69	0.296
	Vidisha	Wheat	191	170	227	✓	✓	90.75	165	160	✓	✓	✓	✓	0.82	370	0.78	0.280
Odisha	**Baleshwar**	Rice	71	71	101	✓	✓	88.12	65	32	✓	✓	✓	✓	0.78	970	0.75	**0.077**
	Baragarh	Rice	217	211	220	✓	✓	90.45	170	43	✓	✓	✓	✓	0.73	645	0.72	**0.003**
	Kalahandi	Rice	192	192	269	✓	✓	91.08	160	10	✓	✓	✓	✓	0.69	1510	0.74	**0.082**
Telangana	**Nalgonda**	Rice	298	298	161	✓	✓	87.58	110	82	✓	✓	✓	✓	0.78	489	0.74	0.875
	Nizamabad	Rice	68	68	121	✓	✓	88.43	160	41	✓	✓	✓	✓	0.78	499	0.72	0.134
	Suryapet	Rice	102	102	168	✓	✓	89.29	49	23	✓	✓	✓	✓	0.72	472	0.70	0.990
Uttar Pradesh	**Bahraich**	Wheat	204	200	204	✓	✓	88.24	160	149	✓	✓	✓	✓	0.79	405	0.79	0.903
	Barabanki	Wheat	217	210	232	✓	✓	91.81	161	154	✓	✓	✓	✓	0.76	501	0.76	0.960
	Bareilly	Wheat	169	200	217	✓	✓	89.86	169	135	✓	✓	✓	✓	0.76	356	0.73	0.171
	Deoria	Wheat	232	210	176	✓	✓	86.93	163	147	✓	✓	✓	✓	0.65	316	0.76	**0.026**
	Fatehpur	Wheat	218	200	222	✓	✓	89.19	161	139	✓	✓	✓	✓	0.77	325	0.75	**0.054**
Uttarakhand	**Udamsingh Nagar**	Wheat	196	200	256	✓	✓	92.58	164	147	✓	✓	✓	✓	0.72	294	0.78	0.311
			4644	**4579**	**4839**				**3075**	**2391**								

Annexures

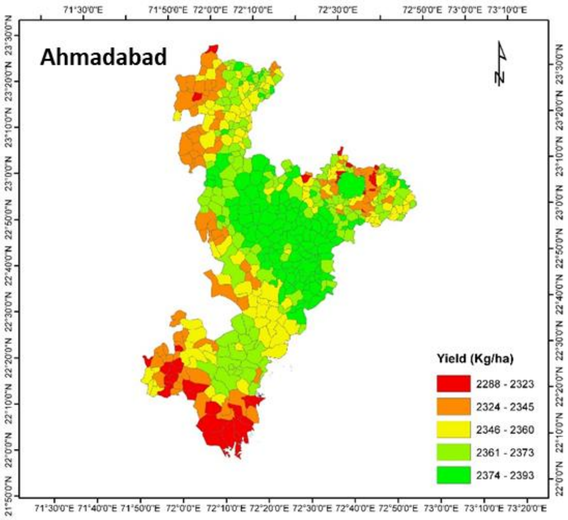
Ahmadabad
Yield (Kg/ha)
2288 - 2323
2324 - 2345
2346 - 2360
2361 - 2373
2374 - 2393

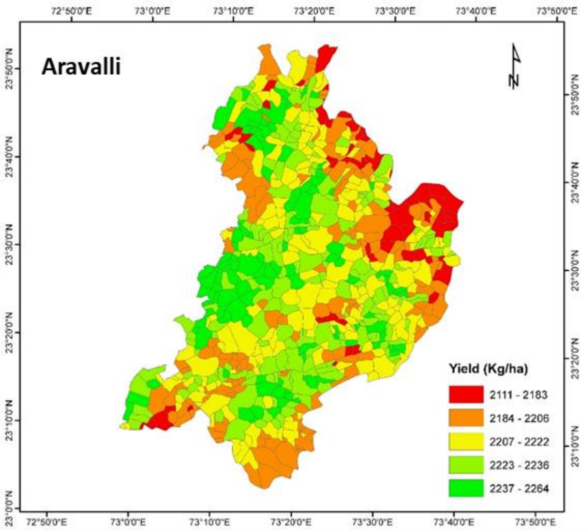
Aravalli
Yield (Kg/ha)
2111 - 2183
2184 - 2206
2207 - 2222
2223 - 2236
2237 - 2264

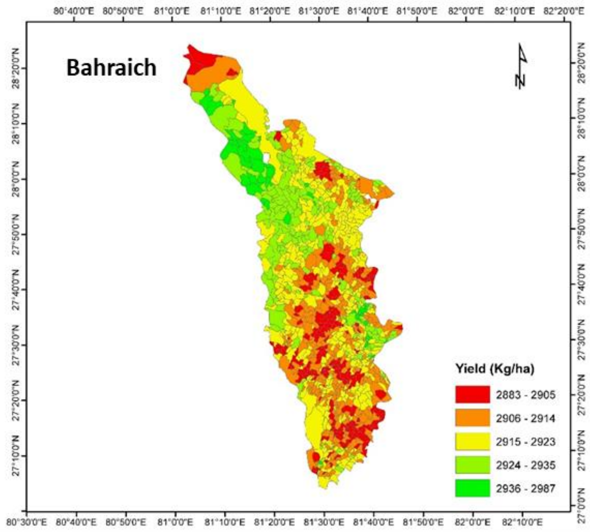
Bahraich
Yield (Kg/ha)
2883 - 2905
2906 - 2914
2915 - 2923
2924 - 2935
2936 - 2987

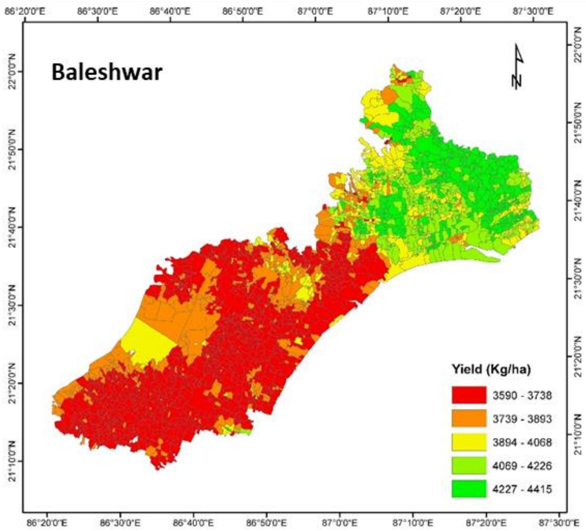
Baleshwar
Yield (Kg/ha)
3590 - 3738
3739 - 3893
3894 - 4068
4069 - 4226
4227 - 4415

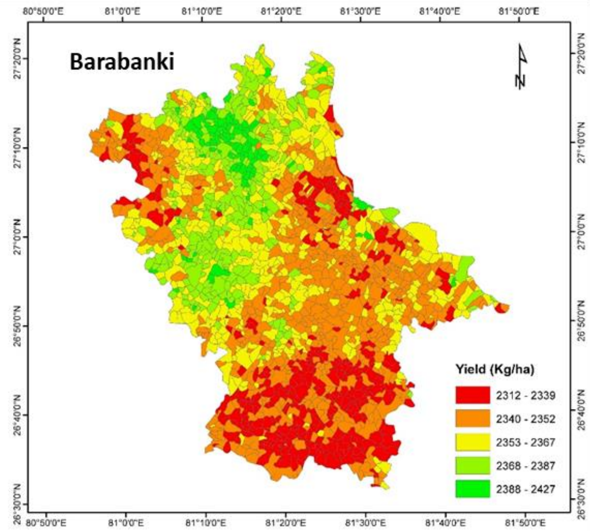
Barabanki
Yield (Kg/ha)
2312 - 2339
2340 - 2352
2353 - 2367
2368 - 2387
2388 - 2427

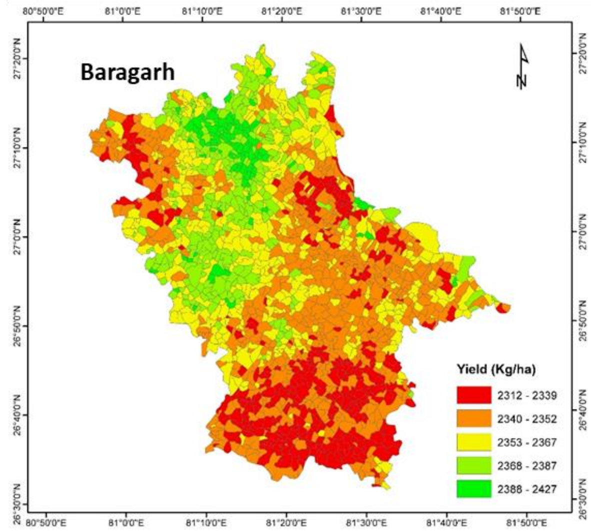
Baragarh
Yield (Kg/ha)
2312 - 2339
2340 - 2352
2353 - 2367
2368 - 2387
2388 - 2427

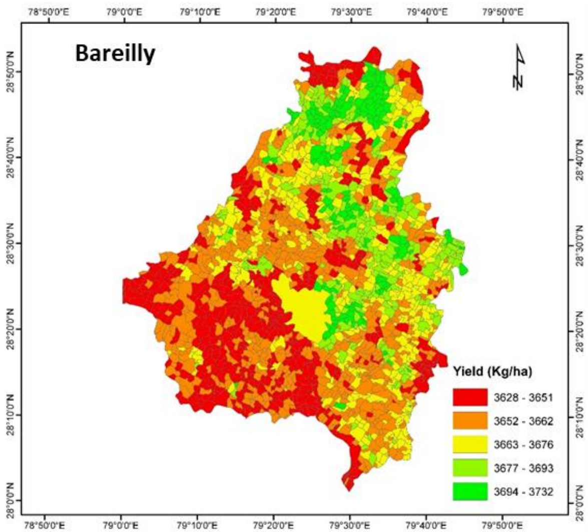
Bareilly
Yield (Kg/ha)
3628 - 3651
3652 - 3662
3663 - 3676
3677 - 3693
3694 - 3732

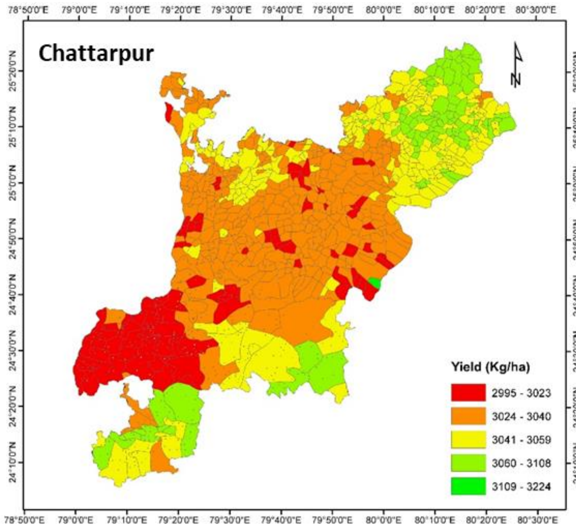
Chattarpur
Yield (Kg/ha)
2995 - 3023
3024 - 3040
3041 - 3059
3060 - 3108
3109 - 3224

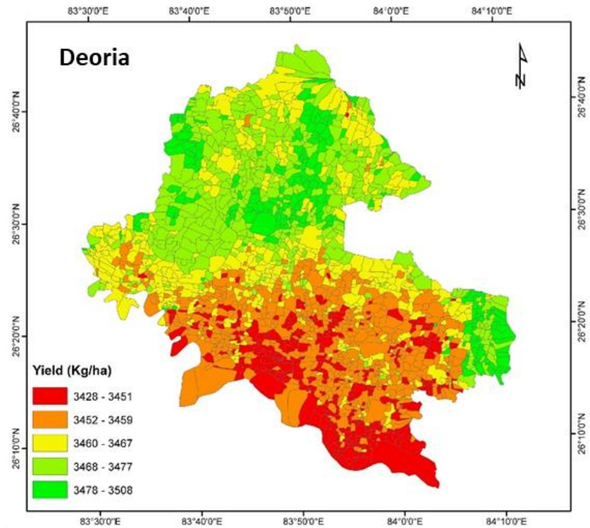
Deoria
Yield (Kg/ha)
3428 - 3451
3452 - 3459
3460 - 3467
3468 - 3477
3478 - 3508

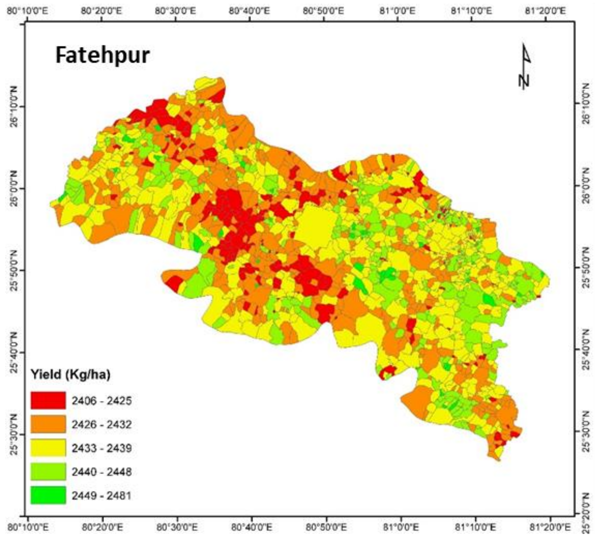
Fatehpur
Yield (Kg/ha)
2406 - 2425
2426 - 2432
2433 - 2439
2440 - 2448
2449 - 2481

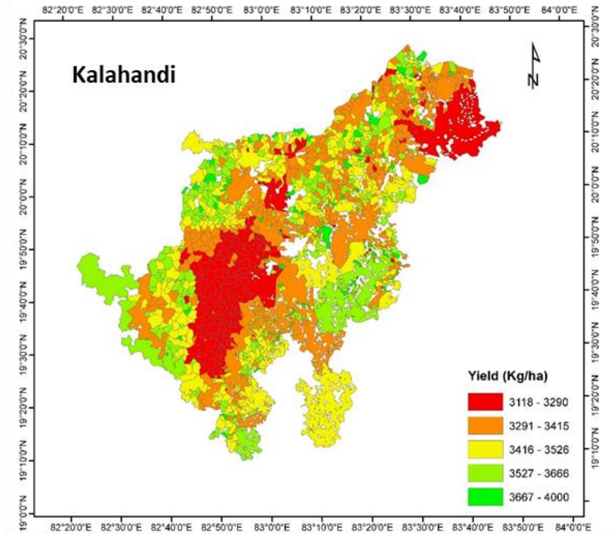
Kalahandi
Yield (Kg/ha)
3118 - 3290
3291 - 3415
3416 - 3526
3527 - 3666
3667 - 4000

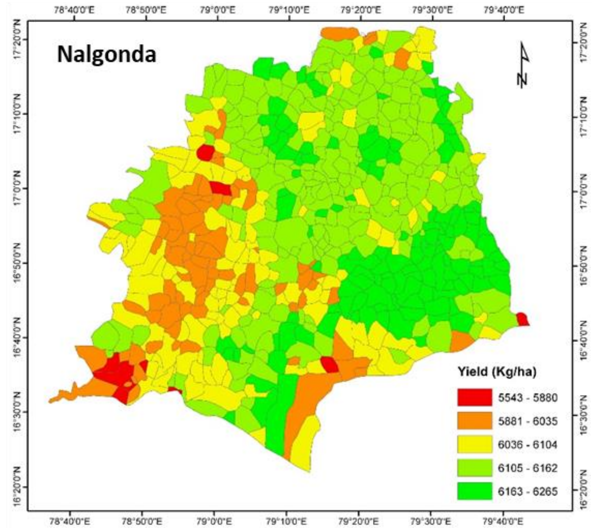
Nalgonda
Yield (Kg/ha)
5543 - 5880
5881 - 6035
6036 - 6104
6105 - 6162
6163 - 6265

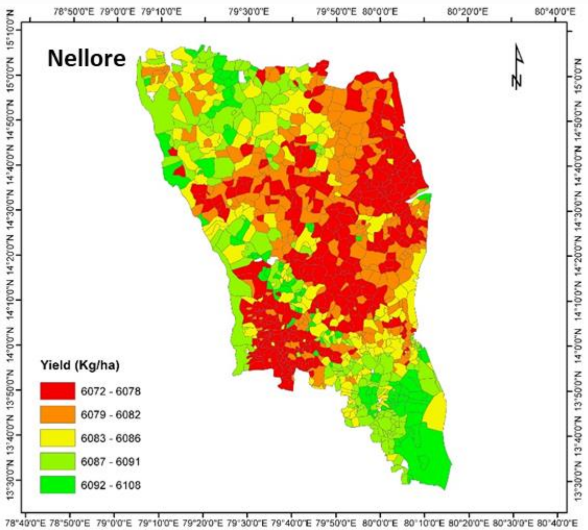
Nellore
Yield (Kg/ha)
6072 - 6078
6079 - 6082
6083 - 6086
6087 - 6091
6092 - 6108

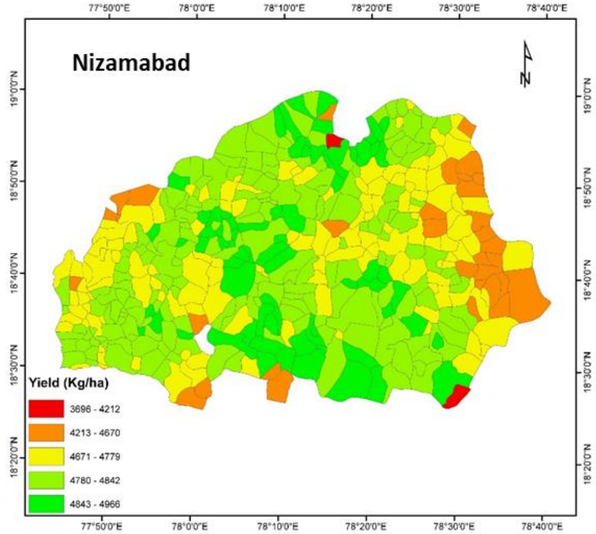
Nizamabad
Yield (Kg/ha)
3696 - 4212
4213 - 4670
4671 - 4779
4780 - 4842
4843 - 4966

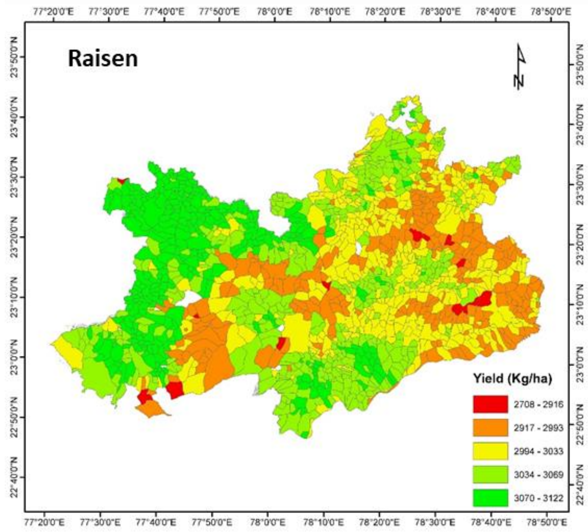
Raisen
Yield (Kg/ha)
2708 - 2916
2917 - 2993
2994 - 3033
3034 - 3069
3070 - 3122

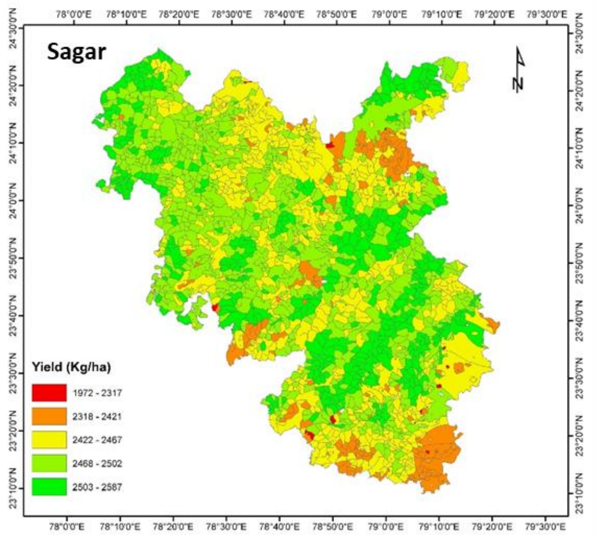
Sagar
Yield (Kg/ha)
1972 - 2317
2318 - 2421
2422 - 2467
2468 - 2502
2503 - 2587

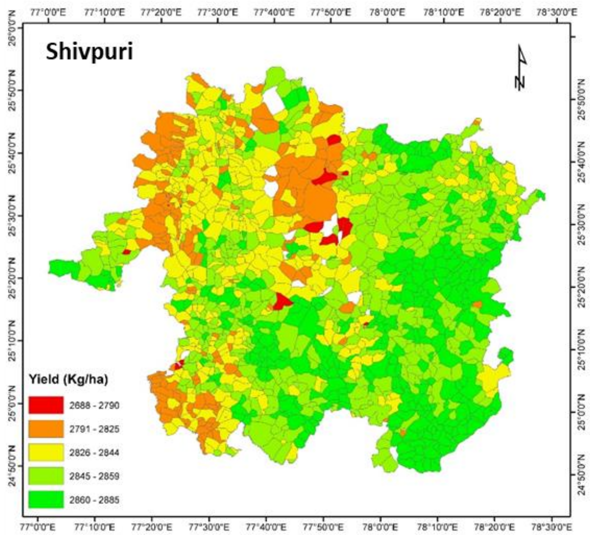
Shivpuri
Yield (Kg/ha)
2688 - 2790
2791 - 2825
2826 - 2844
2845 - 2859
2860 - 2885

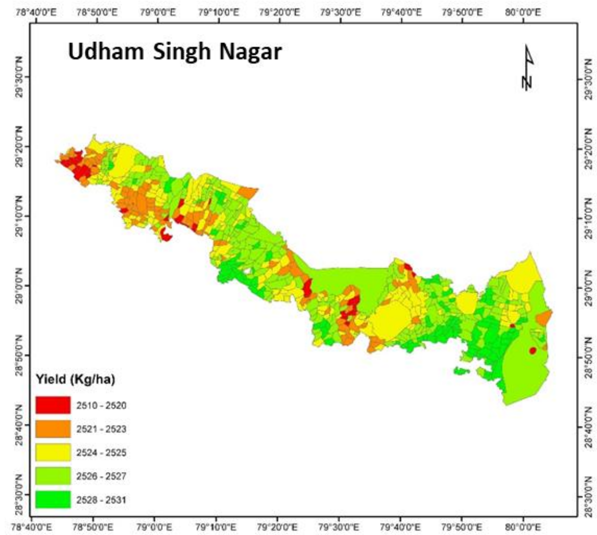
Udham Singh Nagar
Yield (Kg/ha)
2510 - 2520
2521 - 2523
2524 - 2525
2526 - 2527
2528 - 2531

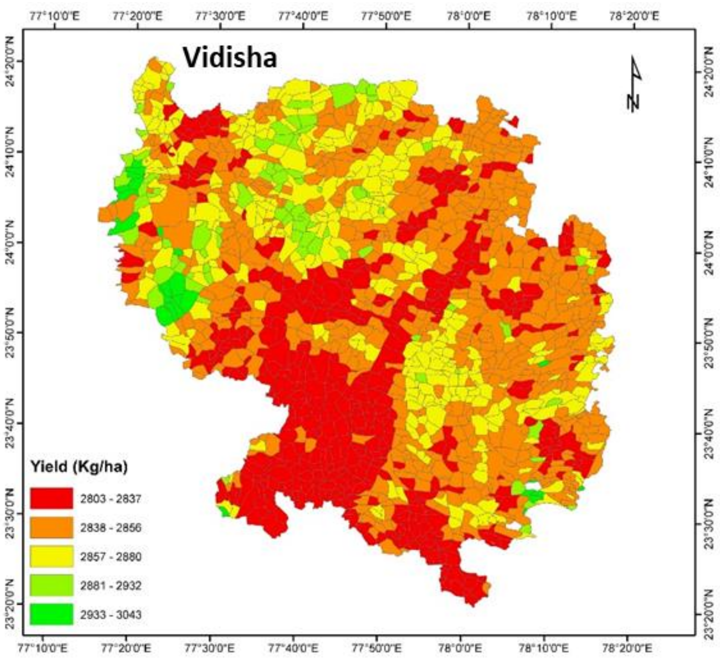

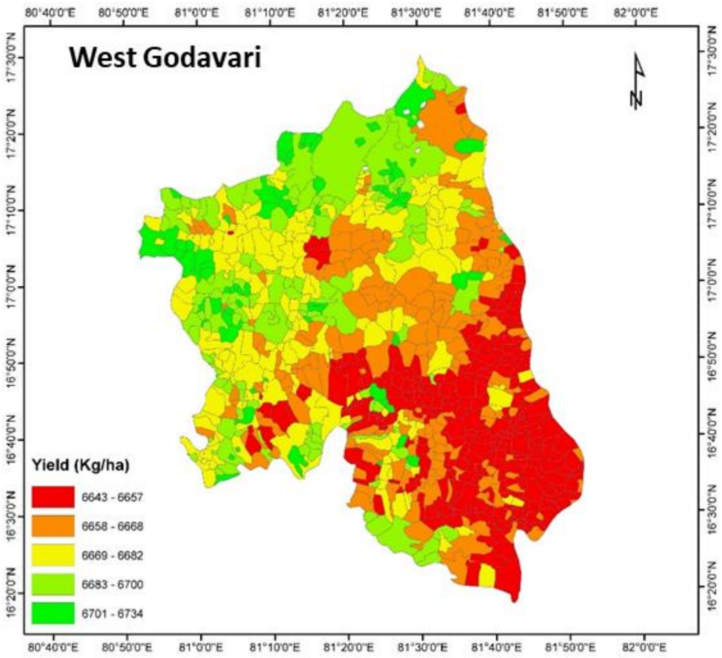

References

Doraiswamy, P. C., Moulin, S., Cook, P. W., & Stern, A. (2003). Crop yield assessment from remote sensing. *Photogrammetric engineering & remote sensing, 69*(6), 665-674.

Fang, H., Liang, S., & Hoogenboom, G. (2011). Integration of MODIS LAI and vegetation index products with the CSM–CERES–Maize model for corn yield estimation. *International Journal of Remote Sensing, 32*(4), 1039-1065.

Gumma, M. K., Thenkabail, P. S., Deevi, K. C., Mohammed, I. A., Teluguntla, P., Oliphant, A., . . . Whitbread, A. M. (2018). Mapping cropland fallow areas in myanmar to scale up sustainable intensification of pulse crops in the farming system. *GIScience & Remote Sensing, 55*(6), 926-949. doi:10.1080/15481603.2018.1482855

Gumma, M. K., Thenkabail, P. S., Teluguntla, P., Rao, M. N., Mohammed, I. A., & Whitbread, A. M. (2016). Mapping rice-fallow cropland areas for short-season grain legumes intensification in South Asia using MODIS 250 m time-series data. *International Journal of Digital Earth, 9*(10), 981-1003.

Gumma, M. K., Thenkabail, P. S., Teluguntla, P., & Whitbread, A. M. (2018). Monitoring of spatiotemporal dynamics of rabi rice fallows in south Asia using remote sensing. *Geospatial Technologies in Land Resources Mapping, Monitoring and Management*, 425-449.

Gumma, M. K., Thenkabail, P. S., Teluguntla, P. G., Oliphant, A., Xiong, J., Giri, C., . . . Whitbread, A. M. (2020). Agricultural cropland extent and areas of South Asia derived using Landsat satellite 30-m time-series big-data using random forest machine learning algorithms on the Google Earth Engine cloud. *GIScience & Remote Sensing, 57*(3), 302-322.

Gumma, M. K., Tsusaka, T. W., Mohammed, I., Chavula, G., Ganga Rao, N., Okori, P., . . . Whitbread, A. (2019). Monitoring changes in the cultivation of pigeonpea and groundnut in Malawi using time series satellite imagery for sustainable food systems. *Remote Sensing, 11*(12), 1475.

Gumma, M. K., Uppala, D., Mohammed, I. A., Whitbread, A. M., & Mohammed, I. R. (2015). Mapping Direct Seeded Rice in Raichur District of Karnataka, India. *Photogrammetric Engineering & Remote Sensing, 81*(11), 873-880.

Jin, X., Li, Z., Yang, G., Yang, H., Feng, H., Xu, X., . . . Luo, J. (2017). Winter wheat yield estimation based on multi-source medium resolution optical and radar imaging data and the AquaCrop model using the particle swarm optimization algorithm. *ISPRS Journal of Photogrammetry and Remote Sensing, 126*, 24-37.

Olioso, A., Inoue, Y., Ortega-Farias, S., Demarty, J., Wigneron, J.-P., Braud, I., . . . Calvet, J.-C. (2005). Future directions for advanced evapotranspiration modeling: Assimilation of remote sensing data into crop simulation models and SVAT models. *Irrigation and Drainage Systems, 19*(3-4), 377-412.